

1 **Barley RIC157 is involved in RACB-mediated susceptibility to**
2 **powdery mildew**

3 Stefan Engelhardt, Adriana Trutzenberg, Katja Probst, Johanna Hofer,
4 Christopher McCollum, Michaela Kopischke, and Ralph Hückelhoven[#]
5 Phytopathology, TUM School of Life Science Weihenstephan, Technical
6 University of Munich, Emil-Ramann-Str.2, 85354 Freising, Germany

7 [#]Corresponding author: hueckelhoven@wzw.tum.de

8

9 **Abstract**

10 Successful obligate pathogens benefit from host cellular processes. For the
11 biotrophic ascomycete fungus *Blumeria graminis* f.sp. *hordei* (*Bgh*) it has been shown
12 that barley RACB, a small monomeric G-protein (ROP, RHO of plants), is required for
13 full susceptibility to fungal penetration. The susceptibility function of RACB probably
14 lies in its role in cell polarisation, which may be co-opted by the pathogen for invasive
15 ingrowth of its haustorium. However, the actual mechanism of how RACB supports
16 the fungal penetration success is little understood. RIC proteins (ROP-Interactive and
17 CRIB-(Cdc42/Rac Interactive Binding) motif-containing) are considered scaffold
18 proteins which can interact directly with ROPs via a conserved CRIB motif. Here we
19 describe a yet uncharacterised RIC protein, RIC157, which can interact directly with
20 RACB *in planta*. We show that RIC157 undergoes a recruitment from the cytoplasm
21 to the cell periphery in the presence of activated RACB. During fungal infection,
22 RIC157 and activated RACB colocalise at the penetration site, particularly at the
23 haustorial neck. In a RACB-dependent manner, transiently overexpressed RIC157
24 renders barley epidermal cells more susceptible to fungal penetration. This suggests
25 that RIC157 promotes fungal penetration into barley epidermal cells via its function
26 downstream of RACB.

27

28 **Introduction**

29 Plants have developed a multilayered immunity to defend microbial invasion. This
30 consists of pre-formed barriers and induced defences that base on the receptor-
31 mediated recognition of microbe-derived and endogenous elicitors (Boller and Felix
32 2009; Stukenbrock and McDonald 2009). Except for necrotrophs, invading microbes

33 rely to different extents on a living host to establish an infection. With the help of
34 secreted effectors, pathogens undermine plant immune reactions and influence the
35 host metabolism to render their micro-environment more favourable (Białas *et al.*,
36 2018, Han and Kahmann 2019). The co-evolution between microbial effectors and
37 their specific host target molecules can lead to an increase in host specialisation,
38 symbiotic relationships thereby demonstrating extreme examples. Regarding
39 pathogens, especially in genomes of cereal powdery mildew fungi it has been
40 observed that the amount of genes encoding for metabolic enzymes is massively
41 reduced, concomitantly with the proliferation of the putative effector gene pool and
42 transposable elements (Spanu *et al.*, 2010, Wicker *et al.*, 2013, Frantzeskakis *et al.*,
43 2018). Plant targets of these effectors are not necessarily involved in resistance
44 mechanisms, but also in cellular processes that, when controlled by the pathogen,
45 can support the susceptibility towards the invading pathogen. With the current
46 possibilities to use a plethora of different breeding technologies, durable crop
47 resistance based on the loss of these susceptibility gene product functions is within
48 reach (Dangl *et al.* 2013, Engelhardt *et al.*, 2018).

49 Powdery mildew fungi infect a huge variety of monocot and dicot plants causing
50 massive yield losses in crops. The ascomycete fungus *Blumeria graminis* f.sp. *hordei*
51 (*Bgh*) is the specific causal agent of the agronomically important powdery mildew
52 disease on barley (*Hordeum vulgare*) (Jørgensen and Wolfe 1994). As an obligate
53 biotrophic parasite, *Bgh* requires living epidermal cells to complete its life cycle.
54 Airborne conidia germinate on the leaf surface and form an appressorium to
55 penetrate the cuticle and the cell wall with the help of an immense turgor pressure
56 and the release of cell wall-degrading enzymes (McKeen and Rimmer 1973; Schulze-
57 Lefert and Vogel 2000; Hückelhoven and Panstruga 2011). A successful fungal
58 infection is characterised by the formation of a haustorium inside the host cell, which
59 is essential for nutrient uptake and effector protein delivery (Hahn and Mendgen
60 2001, Voegelé *et al.*, 2001, Panstruga and Dodds 2009). The haustorium is
61 separated from the host cytosol by the extrahaustorial matrix and surrounded by the
62 extrahaustorial membrane (EHM), which is continuous with the plant plasma
63 membrane, but differs functionally and biochemically from it (Koh *et al.*, 2005, Inada
64 and Ueda 2014, Kwaaitaal *et al.*, 2017). It is feasible to imagine a pathogen-triggered
65 active contribution of the plant to accommodate the fungal haustorium.

66 ROPs (RHO (RAS homologue) of plants, or RACs, for rat sarcoma (RAS)-related C3
67 botulinum toxin substrate) form a unique subfamily of small monomeric RHO
68 GTPases in plants, since they do not fall into the phylogenetic RHO subclades of
69 RAC, CDC42 and RHO GTPases found in yeast or animals (Brembu *et al.*, 2006). G-
70 proteins are paradigms of molecular switches due to their ability to bind and
71 hydrolyze GTP. The GTP-bound form represents the activated state, and a plasma
72 membrane association of ROP-GTP via posttranslational lipid modifications is
73 required for downstream signalling (Yalovsky 2015). Upon GTP hydrolysis, GDP-
74 bound or nucleotide-free ROPs are inactive in downstream signalling. The cycling
75 between activated and inactive state needs to be spatiotemporally controlled by
76 regulatory partners. Guanine nucleotide exchange factors (GEFs) positively regulate
77 ROP activity by facilitating the GDP/GTP exchange. In plants, three different sorts of
78 ROP GEFs can be distinguished based on their particular GEF domain: PRONE
79 (plant-specific Rop nucleotide exchanger), DHR2 (DOCK homology region 2, found in
80 SPIKE1) and a less well characterized DH-PH domain (B-cell lymphoma homology-
81 pleckstrin homology) described in a plant homolog of human SWAP70 (Berken *et al.*,
82 2005, Meller *et al.*, 2005, Gu *et al.*, 2006, Basu *et al.*, 2008, Yamaguchi and
83 Kawasaki 2012, Yamaguchi *et al.*, 2012, He *et al.*, 2018). The interaction of ROPs
84 with a GTPase Activating Protein (GAP) enhances the intrinsic GTP hydrolysis
85 activity, followed by ROP inactivation (Berken and Wittinghofer 2008). Beside their
86 putative involvement in ROP recycling, Guanine nucleotide Dissociation Inhibitors
87 (GDIs) bind and sequester inactive ROPs in the cytoplasm and are therefore
88 considered negative regulators of ROP activity (Klahre *et al.*, 2006, Boulter and
89 Garcia-Mata 2010). ROPs are involved in the regulation of a multitude of cellular
90 processes. For instance, the cytoskeleton organisation and consequentially cell
91 shape and function is subject to RHO-like GTPase control (Chen and Friml 2014). In
92 *Arabidopsis thaliana* xylem vessels, AtROP11 signaling promotes cell wall apposition
93 and shapes cell wall pit boundaries (Sugiyama *et al.*, 2019). Different ROPs are
94 involved in polar cell growth and even function antagonistically during the generation
95 of *Arabidopsis thaliana* pavement cells (Craddock *et al.*, 2012). Beside cell
96 polarisation and cytoskeleton organisation, ROPs have been also implicated in
97 membrane trafficking and auxin signaling (Yalovsky *et al.*, 2008, Wu *et al.*, 2011).
98 OsRac1 from rice (*Oryza sativa* enhances cell division by regulating OsMAPK6,
99 thereby promoting rice grain yield (Zhang *et al.*, 2019). OsRAC1 has also been

100 demonstrated to regulate immune-related processes like ROS production, defense
101 gene expression and cell death. OsRac1 becomes activated by OsRacGEF1 upon
102 receptor-mediated perception of fungal-derived chitin by OsCEBiP and OsCERK1
103 (Akamatsu *et al.*, 2013). Chitin-perception might also lead to the activation of
104 OsRAC1 by OsSWAP70 (Yamaguchi *et al.*, 2012). Downstream signaling by
105 OsRAC1 is also triggered after recognition of pathogen effector proteins: Plasma
106 membrane-localised Pit, a nucleotide binding-leucine rich repeat resistance (NLR)
107 protein for the rice blast fungus *Magnaporthe oryzae*, associates with DOCK family
108 GEF OsSPK1, thereby likely activating OsRac1 (Kawano *et al.*, 2010, Kawano *et al.*,
109 2014, Wang *et al.*, 2018). A recent report regarding an involvement in defence
110 reactions against rice blast mediated by the NLR protein PID3 (Zhou *et al.*, 2019)
111 opens up the possibility of OsRac1 being a downstream hub of other rice NLR
112 proteins.

113 In the barley-powdery mildew interaction, several barley proteins involved in ROP
114 signaling or ROP activity regulation have been shown to influence fungal penetration
115 success. The barley ROP RACB has been shown to act as susceptibility factor
116 (Schultheiss *et al.*, 2002, Schultheiss *et al.*, 2003, Hoefle *et al.*, 2011). In the absence
117 of the pathogen, RACB appears to be involved in cell polarization processes, as
118 stable RACB silencing affects stomatal subsidiary cell and root hair development
119 (Scheler *et al.*, 2016). The expression of a constitutively activated GTP-bound RACB
120 supported fungal penetration success into barley epidermal cells, whereas silencing
121 RACB by RNA interference (RNAi) renders epidermal cells less susceptible to fungal
122 invasion. Two RACB-interacting proteins have been described as negative regulators
123 of RACB function in susceptibility. First, the Microtubule-Associated ROP-GAP1
124 (MAGAP1) is recruited to the cell periphery by activated RACB and limits
125 susceptibility to powdery mildew likely by enhancing the GTP-hydrolyzing activity of
126 RACB (Hoefle *et al.*, 2011). Second, activated RACB interacts with the cytoplasmic
127 ROP binding kinase1 (RBK1) *in vivo* and enhances its kinase activity *in vitro*
128 (Huesmann *et al.*, 2012). Transient silencing of RBK1 or RBK1-interacting protein
129 SKP1 (type II S-phase kinase1-associated protein) suggested that RBK1 acts in
130 negative regulation of RACB protein stability and hence in disease resistance (Reiner
131 *et al.*, 2016).

132 In order to regulate cellular processes, ROPs need to activate or deactivate
133 downstream executors (otherwise called ROP effectors, which is avoided here to

134 distinguish from pathogen effectors). The interaction to some of these executors is
135 often indirect and achieved via scaffold proteins bridging the activated ROPs to their
136 signal destination targets. Some ROP scaffold proteins have been described so far
137 in detail, RACK1, ICR/RIPs and RICs. Rice RACK1 (Receptor for Activated C-Kinase
138 1) interacts with several proteins in the OsRac1 immune complex supporting a role in
139 rice innate immunity (Nakashima *et al.*, 2008). ICR/RIPs (Interactor of Constitutive
140 Active ROP/ROP Interactive Partners) are required for cell polarity, vesicle trafficking
141 and polar auxin transport (Lavy *et al.*, 2007, Hazak *et al.*, 2014). In barley, RIPa
142 interacts with RAC1 and organizes microtubule arrays in concert with MAGAP1
143 (Hoefle *et al.*, 2020). Barley RIPb interacts directly with RACB and enhances disease
144 susceptibility towards powdery mildew (McCollum *et al.*, 2019 Preprint). RIC (ROP-
145 Interactive and CRIB-domain containing) proteins, another class of scaffold proteins
146 in ROP signaling, share a highly conserved CRIB motif (Cdc42/Rac Interactive
147 Binding motif, Burbelo *et al.*, 1995), which is essential for the direct interaction with
148 ROPs (Wu *et al.*, 2001). The CRIB domain is also present in a subset of ROP GAPs
149 such as barley MAGAP1 (Schaefer *et al.*, 2011; Hoefle *et al.*, 2011). In barley, the
150 knowledge about RIC protein functions is quite limited. RIC171, however, has been
151 shown to not only interact directly with RACB, but also to increase fungal penetration
152 efficiency in barley epidermal cells upon overexpression. Activated RACB recruits
153 RIC171 to the cell periphery and, in the presence of *Bgh*, RIC171 accumulated at the
154 haustorial neck close to the penetration site (Schultheiss *et al.*, 2008). In *Arabidopsis*
155 *thaliana* (At), 11 different RIC proteins have been identified, that do not share
156 common sequence homology outside their CRIB domain (Wu *et al.*, 2001). By
157 directly interacting with AtROPs, AtRIC proteins are involved in numerous cellular
158 processes. During salt stress, AtROP2 regulates microtubule organisation in an
159 AtRIC1-dependent manner (Li *et al.*, 2017). AtRIC1 also interacts with AtROP6 in
160 pavement cells to enhance the ordering of cortical microtubules upon hormonal
161 signals (Fu *et al.*, 2009) and is involved in cell elongation during pavement cell
162 morphogenesis (Higaki *et al.*, 2017). AtRICs counteract each other to a certain extent
163 as well, as seen with AtROP1-interacting AtRIC3 and AtRIC4 during pollen tube
164 growth. AtRIC3 regulates calcium influx and triggers actin depolymerisation, whereas
165 AtRIC4 enhances actin polymerisation (Gu *et al.*, 2005). Light-induced stomatal
166 opening is regulated via the AtROP2-AtRIC7 pathway. AtROP2 and AtRIC7 are likely
167 to impinge on vesicular trafficking by inhibiting AtExo70B1, which results in a

168 diminished stomatal opening (Hong *et al.*, 2016). These examples emphasize the
169 importance of ROP proteins as signaling hubs for various developmental processes
170 as well as the role of RIC proteins in finetuning specific cellular responses.

171 Here we show results on barley RIC157, a CRIB domain-containing protein that
172 interacts CRIB motif-dependently with RACB in yeast and *in planta*. Overexpression
173 of RIC157 increases the powdery mildew penetration efficiency in barley leaf
174 epidermal cells in a RACB-dependent manner. Cytosolic RIC157 is recruited to the
175 cell periphery specifically by activated RACB and both proteins co-localise at the
176 haustorial neck during the compatible interaction with *Bgh*. Our findings indicate a
177 possible role of the RACB-RIC157 signaling module in promoting fungal penetration,
178 thereby increasing susceptibility towards *Bgh*.

179

180 **Results**

181 **Identification of RIC proteins in barley**

182 Except for a couple of amino acids, individual RIC proteins typically show a lack of
183 primary sequence homology to other proteins in the database outside their CRIB
184 domain (Wu *et al.*, 2001). The highly conserved CRIB motif has been shown to
185 interact directly with activated small RHO GTPases (Burbelo *et al.*, 1995, Aspenström
186 1999). In order to identify additional RIC proteins in barley, we performed a BLAST
187 search using the CRIB motif of previously described RACB interacting protein
188 RIC171 (Schultheiss *et al.*, 2008) against the 2019 annotation of all barley coding
189 sequences (Barley all CDS Morex v2.0 2019, [https://webblast.ipk-
190 gatersleben.de/barley_ibsc/](https://webblast.ipk-gatersleben.de/barley_ibsc/)). Beside RIC171, we identified another seven proteins
191 sharing the properties of RIC proteins, and named them according to their predicted
192 amino acid sequence length RIC153 (HORVU.MOREX.r2.3HG0258770), RIC157
193 (HORVU.MOREX.r2.6HG0469110), RIC163 (HORVU.MOREX.r2.5HG0443720),
194 RIC168 (HORVU.MOREX.r2.2HG0170820), RIC170
195 (HORVU.MOREX.r2.6HG0521090), RIC171 (HORVU.MOREX.r2.2HG0164690),
196 RIC194 (HORVU.MOREX.r2.3HG0258620), RIC236
197 (HORVU.MOREX.r2.2HG0122110). An amino acid sequence alignment of all eight
198 barley RIC proteins illustrated no general domain homologies outside the highly
199 conserved CRIB motif (Fig. 1). Interestingly, the CRIB motif was more C-terminally
200 located in RICs 153, 163 and 194, similar to RIC2 and RIC4 of *Arabidopsis thaliana*
201 (Wu *et al.*, 2001), while the other RICs (157, 168, 170, 171 and 236) contained the

202 CRIB motif closer to their N-terminal end. However, we didn't identify additional
203 conserved domains shared by all members of the barley RIC protein family.
204 RACB-mediated susceptibility towards powdery mildew is determined exclusively in
205 barley leaf epidermal cells. Hence, in order to unravel downstream signaling
206 components of RACB, we focused on barley leaf-expressed RIC proteins. Using
207 online available gene expression databases ([https://webblast.ipk-](https://webblast.ipk-gatersleben.de/barley_ibsc/)
208 [gatersleben.de/barley_ibsc/](https://webblast.ipk-gatersleben.de/barley_ibsc/)), we identified five leaf-expressed *RIC* genes (*RIC153*,
209 *RIC157*, *RIC163*, *RIC194* and previously published *RIC171* (Schultheiss *et al.*, 2008).
210 Despite there is little sequence conservation between RIC proteins outside their
211 CRIB domain, we compared primary sequences of barley, *Arabidopsis thaliana* and
212 rice (*Oryza sativa*) RICs using an available online amino acid motif discovery
213 software (<http://meme-suite.org/tools/meme>). This discovered three previously non-
214 described amino acid motifs shared by individual barley (*RIC157*, *RIC168*, *RIC171*),
215 rice (*Os02g06660.1*, *Os04g53580.1*) and *Arabidopsis* RICs (*RIC10*, *RIC11*) (Suppl.
216 Fig. S1) but not by all RIC proteins.

217

218 **RIC157 increases susceptibility of barley towards *Bgh* in a RACB-dependent** 219 **manner**

220 To investigate a potential function of *RIC157* during the barley-powdery mildew
221 interaction, we analysed the penetration success of *Bgh* on barley epidermal cells
222 during various conditions (Fig. 2). Single cell transient overexpression of *RIC157* had
223 a strong effect on the penetration success of *Bgh* into barley epidermal cells (Fig.
224 2A). The susceptibility to fungal cell entry increased by about 50% compared to
225 control treatments, an outcome that is reminiscent of susceptibility levels observed
226 after transient overexpression of constitutively activated CARACB(G15V) or *RIC171*
227 (Schultheiss *et al.*, 2003, Schultheiss *et al.*, 2008). We did not observe the opposite
228 effect, meaning a decreased fungal penetration after RNA interference (RNAi)-
229 mediated silencing of *RIC157* compared to control levels (Fig. 2B). To check if this
230 elevated susceptibility of barley epidermal cells after overexpression of *RIC157* is
231 dependent on RACB, we analysed the fungal penetration efficiency by simultaneous
232 transient overexpression of *RIC157* and silencing of endogenous RACB expression
233 via RNAi (Fig. 2C). Interestingly, we did not observe an elevated fungal penetration
234 rate, indicating that *RIC157* increases barley epidermal cell susceptibility in a RACB-
235 dependent manner. We confirmed the efficiency of both RNAi silencing constructs via

236 co-expression of fluorescence tag-labelled targets and ratiometric fluorescence
237 measurements (Suppl. Fig. S2).

238

239 **RIC157 interacts directly with RACB in yeast and *in planta***

240 RACB can directly interact with CRIB motif-containing proteins RIC171 and MAGAP1
241 (Schultheiss *et al.*, 2008, Hoefle *et al.*, 2011). Therefore, it appeared likely that
242 RIC157 can directly interact with RACB via its CRIB domain. We conducted different
243 approaches to test for direct protein-protein interaction between RIC157 and RACB.
244 In a targeted yeast-2-hybrid experiment, we showed that RIC157 directly interacts
245 with RACB and with the constitutively activated CARACB(G15V) mutant, but not with
246 the dominant-negative, GDP-bound DNRACB(T20N) mutant (Fig. 3A). Interestingly,
247 we also observed a certain level of interaction between RIC157 and lower nucleotide
248 affinity RACB mutant DNRACB(D121N). This particular mutation has been shown
249 previously in RAS mutant D119N to behave either in a constitutively activated or a
250 dominant-negative way, depending on the experimental setup (Cool *et al.*, 1999).
251 The direct protein-protein interaction between RIC157 and RACB is dependent on
252 the CRIB motif. RIC157 variants either lacking the CRIB motif completely or
253 containing a CRIB motif that has been mutated at two highly conserved histidine
254 residues (Burbelo *et al.*, 1995, Ash *et al.*, 2003), lose the ability to interact with either
255 RACB form nearly entirely (Suppl. Fig. S3). To substantiate these results, we aimed
256 to prove the fusion protein stability by immunoblotting (Suppl. Fig. S4). While all
257 RACB variants were stably expressed and detectable, we were unable to confirm the
258 stability of RIC157 variants in yeast in most of several independent experiments.
259 Together with the fact that the yeast growth on selective medium was slow but
260 dependent on the RIC157 construct, this suggests a high RIC157 turnover in yeast.
261 In order to investigate the *in planta* interaction between RACB and RIC157, we
262 performed Bimolecular Fluorescence Complementation (BiFC, synonym split-Yellow
263 Fluorescent Protein (YFP)) experiments (Walter *et al.*, 2004). We therefore fused N-
264 terminally N- and C-terminal YFP parts to RIC157 and RACB variants and transiently
265 co-expressed complementary splitYFP fusion proteins in barley epidermal cells via
266 particle bombardment. YFP fluorescence reconstitution was ratiometrically quantified
267 against a co-expressed cytosolic mCherry fluorescence marker. As shown in Suppl.
268 Fig. S5, YFP fluorescence was reconstituted to a significantly higher extent when
269 split-YFP fusions of RIC157 were co-expressed with split-YFP fusions of RACB and

270 CARACB(G15V), compared to co-expressions with DNRACB(T20N) and
271 DNRACB(D121N). This suggests that RIC157 might preferentially interact with
272 activated RACB *in planta*. We confirmed the stability of split-YFP fusion proteins via
273 immunoblot analysis of total protein samples extracted from transformed barley
274 mesophyll protoplasts (Suppl. Fig. S5B).

275 Since split-YFP experiments do not unequivocally reveal direct protein-protein
276 interaction, we further analysed the interaction between RACB and RIC157 by FLIM-
277 FRET and in particular the Green Fluorescent Protein (GFP) lifetime reduction (Fig.
278 3B). We fused GFP N-terminally to RIC157 and mCherry N-terminally to different
279 RACB forms and transiently co-expressed respective combinations in barley
280 epidermal cells via particle bombardment. Co-expression of GFP-RIC157 and free
281 mCherry resulted in an average GFP lifetime of about 2.6 ns and is representative of
282 a non-FRET negative control setup. GFP lifetime was slightly lower compared to the
283 negative control samples in cells co-expressing GFP-RIC157 and mCherry-
284 DNRACB(T20N). In contrast to that, the co-expression of GFP-RIC157 with mCherry-
285 CARACB(G15V) led to a strong and highly significant reduction in GFP lifetime to
286 approximately 2.2 ns. This GFP lifetime reduction clearly demonstrates a direct
287 protein-protein interaction between RIC157 and activated RACB *in planta*. A very
288 similar reduction in GFP lifetime we observed when GFP-RIC157 was co-expressed
289 with mCherry-RACB suggesting an interaction of RIC157 with the wildtype form of
290 RACB. The FLIM approach also indicated an interaction of RIC157 with the lower
291 nucleotide affinity RACB mutant DNRACB(D121N). However, the spreading of the
292 single data points was immense from no GFP lifetime reduction down to GFP lifetime
293 reductions reminiscent of mCherry-CARACB(G15V)-expressing cells. Since the
294 D121N mutation leads to a lower nucleotide affinity, this particular result we see here
295 might have been provoked by different physiological cell conditions which in some
296 cells stabilize the GDP-bound, inactive form and in others the GTP-bound, activated
297 form of the DNRACB(D121N) mutant. In total, these different experimental
298 approaches strongly suggest the direct protein-protein interaction between RIC157
299 and the activated form of RACB.

300

301 **Recruitment of RIC157 to the cell periphery is RACB dependent**

302 To investigate the subcellular localisation of RIC157, we fused GFP N-terminally to
303 RIC157 and transiently expressed this construct in barley epidermal cells via biolistic

304 transformation. As shown in Figure 4A (upper row), RIC157 localises to the cytosol,
305 but a lack of GFP fluorescence in the nucleoplasm indicated that GFP-RIC157 is
306 excluded from the nucleus. However, we repeatedly observed a strong fluorescent
307 signal around the nucleus suggesting a potential affinity of RIC157 to the nuclear
308 envelope/endoplasmic reticulum membrane or proteins associated to it.

309 Since we found a direct protein-protein interaction between RIC157 and RACB, we
310 checked the potential impact of RACB on the subcellular localisation of RIC157 by
311 transiently co-expressing GFP-RIC157 with various untagged forms of RACB (Suppl.
312 Fig. S6). The cytoplasmic localisation of RIC157 is not significantly affected in the
313 presence of RACB or the lower nucleotide affinity dominant negative
314 DNRACB(D121N) mutant. However, we observed a decrease in cytoplasmic and
315 nuclear envelope-localised GFP fluorescence and an accumulation of GFP
316 fluorescence at the cell periphery when GFP-RIC157 was co-expressed with the
317 constitutively activated CARACB(G15V) form.

318 Because untagged proteins cannot be properly monitored, we extended our analysis
319 in barley epidermal cells using mCherry-tagged RACB forms (Fig. 4A). Similarly, we
320 detected GFP-RIC157 in the cytoplasm where it co-localised with mCherry fusions of
321 RACB and DNRACB(D121N). In contrast to that, as with the untagged activated
322 RACB, we detected a similarly strong re-localisation of GFP-RIC157 to the cell
323 periphery in the presence of mCherry-tagged CARACB(G15V) that likewise
324 accumulated at this site. This suggests that activated RACB, like other ROPs
325 associating with the plasma membrane probably via its C-terminal prenylation and
326 possible palmitoylation (Schultheiss *et al.*, 2003; Yalovsky 2015), recruits RIC157 to
327 the cell periphery.

328 In order to check if this RIC157 recruitment to the cell periphery is indeed due to the
329 co-expression with activated RACB, we simultaneously transformed barley epidermal
330 cells with a RNAi construct to silence RACB (Fig. 4B). Without RACB silencing, co-
331 expression of GFP-RIC157 and mCherry-CARACB(G15V) again lead to
332 accumulation of both fusions proteins at the cell periphery. RNAi-mediated silencing
333 of RACB on the other hand did not only diminish the mCherry fluorescence to almost
334 non-detectable levels demonstrating RACB silencing took place, it also decreased
335 GFP fluorescence at the cell periphery and increases GFP fluorescence in the
336 cytoplasm. This result clearly supports that the observed recruitment of RIC157 to the
337 cell periphery is mediated by activated RACB. To further confirm the recruitment of

338 RIC157 by activated RACB from the cytoplasm to the plasma membrane, we took
339 advantage of a mCherry-tagged plasma membrane marker, pm-rk (Nelson *et al.*,
340 2007), and analysed the potential co-localization of GFP-RIC157 with pm-rk in the
341 absence and presence of co-overexpressed non-tagged constitutively activated
342 RACB (CARACB(G15V), Suppl. Fig. S7). In the presence of activated RACB,
343 fluorescence signals of GFP and mCherry overlapped to a higher extent compared to
344 an experimental setup lacking overexpressed activated RACB. This unambiguously
345 supports our previous findings that RIC157 is recruited by activated RACB to cell
346 peripheral and plasma-membrane associated localisations.

347 Fluorescent proteins potentially have an impact on the functionality of the proteins to
348 which they are fused due to conformational hindrances. In order to rule out that
349 RIC157 fused to fluorescent proteins behaves differently than untagged RIC157, we
350 analysed the penetration ability of *Bgh* in barley epidermal cells overexpressing GFP-
351 tagged RIC157 (Fig. 2D). The powdery mildew fungus benefited from the presence of
352 GFP-RIC157, similar to untagged RIC157, suggesting that GFP fusion to RIC157 did
353 not prevent its ability to enhance susceptibility towards *Bgh* infection. Moreover, this
354 supports that localisation of N-terminally tagged RIC157 proteins that we observe,
355 represents the localization of a functional RIC157 protein.

356

357 **RIC157 and RACB co-localise and accumulate at penetration site**

358 Co-localisation experiments in unchallenged barley epidermal cells demonstrated a
359 recruitment of RIC157 to the cell periphery in the presence of activated RACB. In
360 order to investigate if both proteins co-localise at a more specific subcellular site
361 during the interaction with the powdery mildew fungus, we analysed the localisation
362 of transiently co-expressed RIC157 and CARACB(G15V) in epidermal barley cells
363 18-24 hours after inoculation with *Bgh*. As shown in Fig. 5, fluorescent protein fusions
364 of RIC157 and activated RACB accumulate close to the fungal penetration site,
365 forming a cone outlining the neck of a developing haustorial initial. The
366 RIC157/CARACB(G15V) co-localisation was much more defined than the
367 fluorescence signal of simultaneously expressed cytoplasmic mCherry (Fig. 5B),
368 indicating a specific membrane-associated co-localisation in epidermal cells that are
369 successfully penetrated by the fungus.

370

371

372 **Discussion**

373 In the presence of *Bgh*, high activity of the ROP protein RACB appears to be
374 disadvantageous for barley. To date, however, our knowledge about the exact
375 RACB-regulated cellular processes, of which the fungus takes advantage, is still quite
376 limited. Albeit we observed a role of RACB or RACB-interacting proteins in polar cell
377 development and cytoskeleton organization (Opalski *et al.*, 2005; Hoefle *et al.*, 2011;
378 Huesmann *et al.*, 2012; Scheler *et al.*, 2016; Nottensteiner *et al.*, 2018), a direct
379 mechanistic link between RACB-mediated susceptibility and RACB-regulated
380 cytoskeleton organisation or polar membrane trafficking is still missing. Our studies,
381 however, open up the prospect of a RACB-regulated pathway via a ROP-specific
382 scaffold protein that might be exploited in barley epidermal cells by *Bgh* to support
383 susceptibility towards powdery mildew.

384

385 **RIC proteins as scaffolds in RACB downstream signalling**

386 In a signaling cascade, scaffold proteins are as vital for mediating the molecular
387 response as upstream signaling hubs or downstream executors. These scaffolds
388 establish not just a hub-executor connection, by doing so they represent also the first
389 branching point in the signalling cascade that eventually leads to specific effects
390 without possessing any kind of enzymatic activity themselves (Zeke *et al.*, 2009,
391 Good *et al.* 2011). Regarding signaling pathways, ROPs function as signaling hubs
392 and have been shown to be involved in loads of cellular processes, and for some
393 ROPs the regulatory role in different, sometimes even antagonistic signalling
394 pathways has been described (Gu *et al.*, 2005, Nibau *et al.*, 2006, Feiguelman *et al.*,
395 2018). If ROPs do not interact directly with downstream executors, RIC proteins (and
396 also ICRs/RIPs, Feiguelman *et al.*, 2018) are considered bridging units creating the
397 scaffold for specific branches of ROP signaling (Schultheiss *et al.*, 2008, Craddock *et al.*,
398 2012, Zhou *et al.*, 2015, Hong *et al.*, 2016). Besides RIC171 and RIC157, we
399 identified another six proteins of different sizes in barley that, by the above-
400 mentioned definition, we consider RIC proteins. Potentially, there is a difference
401 between monocots and dicots regarding the number of RIC proteins, which is
402 slightly higher in Arabidopsis (Wu *et al.*, 2001), suggesting a higher probability of
403 either functional redundancies, diversification or antagonistic partners in dicots (Gu *et al.*,
404 2005). Redundancies between the barley leaf-expressed RIC proteins is,
405 considering the low primary sequence conservation, hard to predict and not known

406 yet. The partial similarities between leaf-expressed RIC157 and RIC171 (Suppl. Fig.
407 1) could, however, indicate functions in similar signaling pathways.

408

409 **RIC157 increases susceptibility towards powdery mildew**

410 In this study, we concentrated on leaf-expressed RIC157 and show, that the transient
411 RIC157 overexpression leads to a strong increase in barley epidermal cell
412 susceptibility towards powdery mildew infection (Fig. 2A). Thus, the fungus benefits
413 from a highly abundant RIC157. The RNA interference-mediated silencing of RIC157,
414 however, did not lead to a higher resistance compared to control-treated cells (Fig.
415 2B). This could have different reasons. Although we have shown a significant
416 reduction of ectopically expressed RIC157 protein levels in the presence of the
417 RIC157 RNAi silencing construct (Suppl. Fig. S2), it must be noted that RNAi-based
418 silencing is never 100% efficient. Remaining endogenous RIC157 transcript levels
419 might be sufficient to allow for control level penetration efficiencies. Additionally, the
420 protein turnover rate of RIC157 is unknown, meaning even with a high RNAi silencing
421 efficiency it is still possible that RIC157 protein, expressed before transient
422 transformation with the RNAi silencing construct, is present throughout the infection
423 assay and sufficiently abundant to support penetration. Another very important point
424 that needs to be stressed is the function of RACB or ROPs in general as signaling
425 hubs (Nibau *et al.*, 2006). The signaling via RIC157 is likely not the only RACB-
426 regulated path that leads to susceptibility. Shutting down the particular RACB-RIC157
427 route probably still leaves other RACB signaling branches functional, which are
428 potentially involved to a certain extent in RACB-mediated susceptibility as well. An
429 increased resistance towards fungal infection was, however, achieved once the
430 signaling hub was removed or switched off by silencing RACB or by transient
431 overexpression of its presumable antagonist MAGAP1 (Schultheiss *et al.*, 2002,
432 Hoefle *et al.*, 2011). In accordance with this, RACB-dependency of the RIC157-
433 promoted susceptibility (Fig. 2C) suggests that even abundant RIC157 still requires
434 the presence of RACB to function as a susceptibility factor.

435

436 **RIC157 interacts with RACB and is recruited to the cell periphery**

437 We have demonstrated that RIC157 can interact directly with RACB in yeast and *in*
438 *planta* (Fig. 3, Suppl. Fig. 5). In barley epidermal cells, RIC157 showed interaction
439 with activated RACB, but not with the dominant negative form. The observed

440 interaction in yeast or via FLIM analysis *in planta* between RIC157 and the dominant-
441 negative form DNRACB(D121N) could be explained by the different experimental
442 setups and/or physiological cell conditions. G-proteins with this particular mutation
443 have been observed previously to display either dominant-negative or constitutively
444 activated properties (Cool *et al.*, 1999). DNRACB(D121N) has an intrinsic lower
445 nucleotide affinity, however in yeast this form could be GTP bound and hence
446 resemble the activated RACB.

447 The subcellular *in planta* CARACB(G15V)-RIC157 interaction site seen in BiFC and
448 FLIM-FRET experiments appeared to be at the cell periphery. This seems
449 conclusive, because RIC157 preferentially interacted with activated RACB. Activated
450 ROPs are supposed to be associated with negatively charged phospholipids in
451 plasmamembrane nanodomains, which is additionally promoted via posttranslational
452 prenylation and S-acylation (Yalovsky 2015, Platre *et al.*, 2019). In *Arabidopsis*
453 *thaliana* it has even been recently shown that particular phosphoinositides are
454 recruited by filamentous pathogens to the plant-microbe interface (Qin *et al.*, 2020),
455 suggesting a similar mechanism during powdery mildew infection of barley.
456 Fluorescence-tagged RIC157 alone did not show any specific localisation in the
457 absence of the fungus, although it seems to be excluded from the nucleus (Fig. 4). In
458 the presence of activated RACB, however, RIC157 undergoes a relocalisation from
459 the cytoplasm to the cell periphery/plasma membrane, where the interaction with the
460 activated ROP takes place. It had previously been shown that expression of activated
461 GFP-RACB alone leads to its preferential localisation at the cell periphery with a
462 cytosolic background (Schultheiss *et al.*, 2003). We assume that a potential influence
463 of endogenous levels of RIC157 or activated RACB on the localisation of their
464 overexpressed interaction partner is probably negligible in our experimental setup. A
465 similar recruitment to the cell periphery has been observed with other proteins that
466 directly interact with activated RACB (Schultheiss *et al.*, 2008, Hoefle *et al.*, 2011,
467 Huesmann *et al.*, 2012, McCollum *et al.*, 2019 Preprint), reinforcing the model that
468 RACB activation is preceding the recruitment of interaction partners and that
469 downstream RACB signaling is initiated at the plasma membrane. This is further
470 supported since a RACB mutant version lacking the C-terminal CSIL motif for
471 prenylation localizes to the cytoplasm and is inactive in promoting susceptibility
472 (Schultheiss *et al.*, 2003).

473 With regard to RACB's and RIC157's capability to support fungal infection, the
474 recruitment of RIC157 to the cell periphery becomes even more interesting. Our data
475 suggest a recruitment of RIC157 to the fungal penetration site (Fig. 5). The cone-like
476 structure surrounding the haustorial neck indicates a subcellular co-localisation with
477 activated RACB. However, the co-localisation of RACB and fungal infection-
478 supporting RACB-interactors is not exclusive to RIC157. RIC171 and RIPb, two
479 proteins also considered scaffolds in RACB signalling, co-localise with RACB at the
480 haustorial neck (Schultheiss *et al.*, 2008, Hückelhoven and Panstruga 2011,
481 McCollum *et al.*, 2019 Preprint). Future experiments may show, whether subcellular
482 co-concentration of RACB and RACB-interacting proteins indicate a specific lipid
483 composition of the haustorial neck, which then recruits activated ROPs, or a
484 membrane domain of high ROP activity due to local GEF activity, or perhaps
485 indicates an exclusion of ROPs from further lateral diffusion into the EHM, which was
486 suggested to be controlled at the haustorial neck (Koh *et al.*, 2005).

487

488 **RIC157 and susceptibility**

489 RIC157 transiently overexpressed in barley epidermal cells localises to the cytoplasm
490 and enhances fungal penetration efficiency in a RACB-dependent manner. Activated
491 RACB, however, associates with the plasma membrane where it likely recruits
492 RIC157 for downstream signaling. Thus, transiently overexpressed and endogenous
493 RIC157 might promote RACB-mediated susceptibility upon recruitment to the cell
494 periphery by endogenously present activated RACB. Only a small fraction of
495 overexpressed RIC157 is possibly recruited to the cell periphery without concomitant
496 co-overexpression of activated RACB. This means that such a minute fluorescence
497 localisation change might be probably undetectable in our experimental setup, but it
498 needs to be emphasized that we do not assume RIC157 promoting susceptibility to
499 powdery mildew from a solely cytoplasmic site. Indeed, in front of a cytoplasmic
500 background, RIC157 is also visible at the cell periphery without co-expression of
501 CARACB(G15V), possibly reflecting partial recruitment by endogenous ROPs (Fig.
502 4A).

503 The domain and sequence similarity between barley RIC157 and *Arabidopsis*
504 *thaliana* RIC10 and RIC11 (Suppl. Fig. 1) does not necessarily indicate similar
505 functions of both proteins. Beside AtRIC10 and AtRIC11, for which nothing is known
506 to date about their biological function, RIC157 also shares limited amino acid motif

507 similarity with AtRIC1, AtRIC3 and AtRIC7 (Suppl. Fig. 8), for which an involvement
508 in cytoskeleton organization has previously been demonstrated. From these three
509 Arabidopsis RIC proteins, AtRIC1 appears to be an interesting candidate from which
510 a RIC157 function could be deduced. AtRIC1 has been shown to interact with ROP6
511 to activate the p60 subunit of Katanin, a microtubule-severing enzyme (Lin *et al.*,
512 2013), as opposed to the interaction with AtROP2 that negatively regulates the action
513 of AtRIC1 on microtubules (Fu *et al.*, 2005). The microtubule-severing activity of
514 Katanin might even be regulated by AtROP2, AtROP4 and AtROP6 (Ren *et al.*, 2017)
515 via AtRIC1. Whether barley RIC157 also fulfils such a regulatory role in organising
516 microtubules still remains to be seen. Regarding the subcellular localisation there
517 are, however, clear differences: Barley RIC157 localises to the cytoplasm, AtRIC1
518 associates with microtubules (Fu *et al.*, 2005). However, when microtubule arrays in
519 penetrated and attacked but non-penetrated barley epidermal cells were compared,
520 penetration success was strongly associated with parallel non-polarized microtubule
521 arrays in the cell cortex and a diffuse or depleted microtubule structure at the
522 haustorial neck (Hoefle *et al.*, 2011). AtRIC3 has been shown to be involved in the
523 pollen tube growth process, where its function leads to actin disassembly in a ROP1-
524 dependent manner upon calcium influx into the cytoplasm (Gu *et al.*, 2005, Lee *et al.*,
525 2008). Likewise, AtRIC7 was recently reported to influence vesicle trafficking in
526 stomata resulting in the suppression of an elevated stomatal opening after ROP2-
527 dependent inhibition of the exocyst complex *via* Exo70B1 (Hong *et al.*, 2016). Both F-
528 actin organization and exocyst function are important in penetration resistance to *Bgh*
529 (Opalski *et al.*, 2005, Miklis *et al.*, 2007, Ostertag *et al.*, 2012). Therefore, the
530 discovery of RIC157 as a RACB-dependent susceptibility factor may pave the way to
531 a better understanding of ROP-steered processes that are pivotal for fungal invasion
532 into barley epidermal cells. The challenge will be to find the downstream factors that
533 RIC157 activates and to understand how RIC157 interacts with RACB in the
534 presence of several other RACB interactors. We assume that several diverse RICs
535 and ICR/RIP proteins could form a cooperative network for orchestrating F-actin,
536 microtubule and membrane organization at the site of fungal entry.

537

538 **Experimental procedures**

539 **Plant and fungal growth conditions**

540 Wildtype barley (*Hordeum vulgare*, cultivar „Golden Promise“) was cultivated in long
541 day conditions (16 hours day light, 8 hours darkness) at a temperature of 18°C with a
542 relative humidity of 65% and a light intensity of 150 $\mu\text{mol s}^{-1} \text{m}^{-2}$.

543 The biotrophic powdery mildew fungus *Blumeria graminis* f.sp. *hordei* A6 was used in
544 all experiments. It was cultivated and propagated on barley „Golden Promise“ under
545 the same condition described above.

546

547 **Cloning of constructs**

548 Via a Two-Step Gateway cloning approach, in a first PCR *RIC157*
549 (HORVU.MOREX.r2.6HG0469110) was amplified from a barley cDNA pool prepared
550 from leaf and epidermal peels using gene-specific primers *RIC157_GW_for* and
551 *RIC157_GW_rev+STOP* (Suppl. Table 1) creating an incomplete Gateway
552 attachment site overhang. A second PCR using primers *attB1* and *attB2* completed
553 the attachment sites. To create a Gateway entry clone of *RIC157*, the amplified
554 product was recombined into pDONR223 (Invitrogen) via BP-reaction using Gateway
555 BP Clonase™ II according to manufacturer's instruction (Thermo Fisher Scientific).

556 To clone *RIC157 Δ CRIB*, both fragments upstream and downstream of CRIB motif
557 were amplified separately using primers *RIC157_GW_for* and *RIC157delCRIB_rev*
558 for PCR1, *RIC157delCRIB_for* and *RIC157_GW_rev+STOP* for PCR2, creating
559 overlapping overhangs. In PCR3 both fragments together with primers
560 *RIC157_GW_for* and *RIC157_GW_rev+STOP* completed *RIC157 Δ CRIB* with
561 incomplete Gateway attachment sites overhangs. Completion of attachment sites
562 and creating an entry clone in pDONR223 was done as described above. To clone
563 *RIC157-H37Y-H40Y*, a site-directed mutagenesis using primers
564 *CRIB157H37&40Y_for* and *CRIB157H37&40Y_rev* was performed according to
565 QuikChange® Site-Directed Mutagenesis Protocol (Stratagene). For cloning entry
566 constructs of *RACB* variants, primers *RACB_GW_for* and *RACB_GW_rev* were used
567 to amplify *RACB* from previously described constructs (Schultheiss *et al.*, 2003) and
568 cloned into pDONR223 via BP as described above. To clone *DNRACB(D121N)*, a
569 site-directed mutagenesis using primers *RACB_D121N_fw* and *RACB_D121N_rv*
570 was performed according to QuikChange® Site-Directed Mutagenesis Protocol
571 (Stratagene).

572 For RNA interference (RNAi) silencing of *RIC157* in barley, we PCR-amplified two
573 *RIC157* fragments, a 97bp fragment with primers *RIC157_RNAi_NotI_for* and

574 RIC157_RNAi_EcoRI_rev containing NotI and EcoRI restriction sites, and a 324bp
575 fragment with primers RIC157_RNAi_EcoRI_for and RIC157_RNAi_XbaI_rev
576 containing EcoRI and XbaI restriction sites. After restriction digest of all sites, ligating
577 into pIPKTA38 via NotI and XbaI sites we created a *RIC157_RNAi* entry construct
578 lacking the CRIB motif nucleotide sequence to prevent off-target silencing of other
579 CRIB-domain containing RNAs. The *RIC157_RNAi* sequence was then cloned via LR
580 reaction using Gateway LR Clonase™ II according to manufacturer's instruction
581 (Thermo Fisher Scientific) into RNAi expression plasmid pIPKTA30N to create a
582 double-strand RNAi expression construct (Douchkov *et al.*, 2005).

583 For Yeast-2-Hybrid expression clones, entry clones of *RIC157* and *RACB* variants
584 were introduced into prey plasmid pGADT7-GW and pGBKT7-GW via LR reaction
585 using Gateway LR Clonase™ II according to manufacturer's instruction (Thermo
586 Fisher Scientific). pGADT7-GW and pGBKT7-GW have been modified from pGADT7
587 and pGBKT7 (Clontech) into a Gateway-compatible form using Gateway™ Vector
588 Conversion System (Thermo Fisher Scientific). To create *RACB* variants lacking C-
589 terminal prenylation sequence, a premature STOP-Codon was introduced by site-
590 directed mutagenesis as described above using primers delCSIL_for and
591 delCSIL_rev.

592 In order to clone BiFC constructs, we PCR amplified a *RIC157* full-length fragment
593 with primers RIC157_BamHI_for and RIC157_KpnI_rev containing BamHI and KpnI
594 restriction sites. After restriction digest, we ligated this construct into pUC-
595 SPYNE(R)173 (Waadt *et al.*, 2008).

596 For localisation and overexpression studies in barley, *RIC157* and *RACB* variants in
597 pDONR223 were used as entry constructs to clone them into various pGY1-based
598 CaMV35S promoter-driven expression vectors (Schweizer *et al.*, 1999) via LR
599 reaction as described above. Empty pGY1 (encoding for no tag) was rendered
600 Gateway-compatible via Gateway™ Vector Conversion System (Thermo Fisher
601 Scientific). To create expression vectors for proteins C- or N-terminally tagged by
602 GFP or mCherry, Gateway Reading Frame Cassettes for C- and N-terminal fusions,
603 respectively, were integrated into a pGY1-plasmid backbone upon XbaI digestion and
604 combined at 5' or 3' with sequences of monomeric GFP or mCherry. Cloning
605 procedure was performed using In-Fusion HD cloning kit (Takara Bio USA).
606 Constructs for GFP and mCherry upstream or downstream of the Gateway cassette
607 were amplified using primers GW_RfA_mCherry-F, GW_RfA_mGFP-F,

608 GW_RfA_Xba-R, GW_Xba_RfB-F, GW_RfB-R, meGFP-STP-F, mCherry-STP-F,
609 XFP-noSTP_Xba-F, XFP-noSTP-R, meGFP-noSTP-R, mCherry-STP_Xba-R and
610 meGFP-STP_Xba-R.

611 The RACB RNAi construct, RACB BiFC constructs have been described previously
612 (Schultheiss *et al.*, 2003, Schultheiss *et al.*, 2008, Schnepf *et al.*, 2018, McCollum *et*
613 *al.*, 2019 Preprint).

614

615 **Barley epidermal cell transformation and penetration efficiency assessment**

616 For transient overexpression in barley, primary leaf epidermal cells of 7d old plants
617 were transformed using biolistic bombardment with 1µm gold particles that were
618 coated with 2µg of each test plasmid and additionally with 1µg of a cytosolic
619 transformation marker. After mixing the gold particles with plasmid combinations,
620 CaCl₂ (0.5M final concentration) and 3.5µl of 2mg/ml Protamine (Sigma) were added
621 to each sample. The gold particle solution was incubated at room temperature for
622 30min, washed twice with 500µl Ethanol (first 70%, then 100%) and eventually
623 dissolved in 6µl 100% ethanol per biolistic transformation. After shooting, leaves
624 were incubated at 18°C.

625 For localisation and BiFC experiments, leaves were analysed 2 days after
626 transformation. For FRET-FLIM analysis of RACB-RIC157 interaction, barley primary
627 leaves of 7d old plants were transiently transformed. Therefore, 2ug of mCherry-
628 RACB and 1ug meGFP-RIC157 containing plasmids were coated on gold particles
629 for biolistic transformation of single barley epidermal cells.

630 For inoculation with *Bgh*, fungal spores were manually blown in a closed infection
631 device over transformed leaves either 6 hours after transformation (for microscopic
632 analyses 16 hours after inoculation) or 1 day after transformation (to check
633 penetration efficiency 48 hours after inoculation).

634 To analyse penetration efficiency, a transient assay system based on a cytosolic
635 GUS marker was used as described previously (Schweizer *et al.*, 1999). The reporter
636 gene construct pUbiGUSPlus was a gift from Claudia Vickers (Addgene plasmid #
637 64402; <http://n2t.net/addgene:64402>; RRID:Addgene_64402, Vickers *et al.*, 2003).
638 Additionally to overexpression or RNAi silencing constructs, each barley leaf was co-
639 transformed with pUbiGUSPlus. 48 hours after *Bgh* inoculation, leaves were
640 submerged in GUS staining solution (0.1M Na₂HPO₄/NaH₂PO₄ pH 7.0, 0.01 EDTA,
641 0.005M Potassium hexacyanoferrat (II), 0.005M Potassium hexacyanoferrat (III),

642 0.1% (v/v) Triton X-100, 20% (v/v) Methanol, 0.5mg/mL 1.5-bromo-4-chloro-3-
643 indoxyl- β -D-glucuronic acid). For the solution to enter the leaf interior, a vacuum was
644 applied. The leaves were incubated at 37°C over night in GUS staining solution and
645 subsequently for at least 24 hours in 70% Ethanol. Fungal structures were stained
646 with ink-acetate solution (10% ink, 25% acetic acid). Transformed cells were
647 identified after GUS staining with light microscopy. An established haustorium was
648 considered a successful penetration and for each sample at least 50 interactions
649 were analysed. Barley epidermal cells transformed with the empty expression
650 plasmid were used as negative control.

651

652 **Barley protoplast preparation and transformation**

653 To prepare protoplasts from barley mesophyll cells, the lower epidermis of primary
654 leaves from 7 day-old barley plants was peeled and the leaves were incubated 3 to 4
655 hours at room temperature in the darkness while floating with the open mesophyll
656 facing downwards on an enzymatic digestion solution: 0.48M mannitol, 0.3% (w/v)
657 Gamborg B5, 10mM MES pH 5.7, 10mM CaCl₂, 0.5% (w/v) Cellulase R10, 0.5%
658 (w/v) Driselase, 0.5% Macerozyme R10. After enzymatic treatment, an equal amount
659 of W5 solution was added: 125mM CaCl₂, 154mM NaCl, 5mM KCl, 2mM MES pH
660 5.7. Upon filtering through a 40 μ m nylon mesh, the protoplasts were pelleted 5min at
661 200g and carefully resuspended in 10ml W5 solution. After another centrifugation
662 step, the protoplast concentration was adjusted to 2 x 10⁶ cells per mL in MMG
663 solution: 0.4M mannitol, 15mM CaCl₂, 2mM MES pH 5.7. For each transformation
664 sample, 1mL protoplast solution was mixed with 50 μ g of each plasmid and 1.1mL
665 PEG solution (40% (w/v) PEG4000, 0.1M mannitol, 0.2M CaCl₂) and incubated
666 20min at room temperature in the darkness. Afterwards, 4.4mL of W5 solution was
667 added to each transformation and gently mixed. After another pelleting at 200g, the
668 protoplasts were resuspended in 1mL W1 solution (0.5M mannitol, 20mM KCL, 4mM
669 MES pH 5.7) and incubated in the darkness at room temperature for at least 16
670 hours.

671

672 **Yeast-2-Hybrid**

673 Yeast strain AH109 was transformed with bait (pGBKT7) and prey (pGADT7)
674 constructs by following the small scale yeast transformation protocol from
675 YeastmakerTM Yeast Transformation System 2 (Clontech). Upon transformation,

676 yeast cells were plated on Complete Supplement Medium (CSM) plates lacking
677 leucine and tryptophan (LW) and incubated for 3 days at 30°C. A single colony was
678 taken to inoculate 5mL of LW-dropout liquid medium that was incubated with shaking
679 over night at 30°C. The next day, 2mL of culture was pelleted for immunoblot
680 analyses. 7.5µL of undiluted overnight culture (and additionally a 1:10, 1:100 and
681 1:1000 for control purposes) were dropped on CSM plates lacking leucine and
682 tryptophan, and also on CSM plates lacking leucine, tryptophan and adenine. Plates
683 were incubated for at least 3 days at 30°C. Growth on CSM-LW plates confirmed the
684 successful transformation of both bait and prey plasmids, while growth on CSM-
685 LWAd plates indicated activation of reporter genes. As control for a positive and
686 direct protein-protein interaction we routinely used murine p53 and the SV40 large T-
687 antigen (Li and Fields 1993).

688

689 **Immunoblot analysis**

690 For total protein extraction from yeast, we followed the protocol described in
691 Kushnirov (2000) using 2mL of over night culture of yeast transformants grown in
692 CSM-LW liquid medium. The extraction of total protein from barley mesophyll
693 protoplasts was performed by pelleting transformed protoplasts 5min at 200g. The
694 pellet was resuspended thoroughly in 50µL of 2x SDS loading buffer by vortexing. A
695 complete protein denaturation was achieved by boiling protoplast samples 10min at
696 95°C. After shortly spinning down the samples, the stability of fusion proteins in yeast
697 and in planta was assessed via Sodium dodecylsulfate-polyacrylamide gel
698 electrophoresis (SDS-PAGE) and immunoblotting on PVDF membranes. Antibodies
699 used for detecting protein bands on PVDF membranes came from SantaCruz
700 Biotechnology (<https://www.scbt.com/scbt/cart/cart.jsp>): anti-GFP(B-2), anti-
701 cMyc(9E10), anti-HA(F-7) and horseradish-peroxidase conjugated anti-mouse.
702 Presence of antibodies on membrane was visually detected by using SuperSignal
703 West Femto Chemiluminescence substrate (ThermoFisher Scientific). Equal protein
704 loading and blotting success was confirmed via Ponceau S-staining of the PVDF
705 membrane.

706

707 **Microscopy**

708 Localisation and BiFC experiments were analysed on a Leica TCS SP5 confocal
709 laser scanning microscope. The excitation laser wavelengths were 458nm for CFP,

710 488nm for GFP, 514nm for YFP and 561nm for RFP and mCherry, respectively. The
711 fluorescence emission was collected from 462 to 484nm for CFP, from 500-550nm
712 for GFP, from 515 to 550nm for YFP and from 569 to 610nm for RFP and mCherry.
713 Barley epidermal cells were imaged via sequential scanning as z-stacks in 2 μ m
714 increments. Maximum projections of each z-stack were exported as Tiff files from the
715 Leica LAS AF software (version 3.3.0).

716 Localisation experiments of fluorescent protein fusions and BiFC analysis in barley
717 epidermal cells were conducted from 24 hours until 48 hours after biolistic
718 transformation. Regarding ratiometric BiFC quantification using Leica LAS AF
719 software (version 3.3.0), the fluorescence intensity was evaluated over the whole cell
720 area and the ratio between YFP and cytosolic mCherry fluorescence signal was
721 calculated. For each BiFC combination, the fluorescence of at least 20 cells was
722 measured.

723 For FRET-FLIM analysis of RACB-RIC157 interaction, the expression of the
724 fluorophore-fusion proteins was analysed 1 day after transformation using an
725 Olympus FluoView™3000 inverse laser scanning confocal microscope with an
726 UPLSAPO 60XW 60x/NA 1.2/WD 0.28 water immersion objective (Olympus,
727 Hamburg, Germany). Fluorescence of GFP was collected between 500-540nm and
728 mCherry emission was imaged between 580-620nm upon excitation with 488 and
729 561nm argon laser lines, respectively. For FRET-FLIM measurements the PicoQuant
730 advanced FCS/FLIM-FRET/rapidFLIM upgrade kit (PicoQuant, Berlin, Germany) was
731 used, comprising a 485nm pulsed laser line for GFP excitation (pulse rate 40 MHz,
732 laser driver: PDL 828 SEPIA II, laser: LDH-D-C-485), a Hybrid Photomultiplier
733 Detector Assembly 40 to detect GFP fluorescence and a TimeHarp 260 PICO Time-
734 Correlated Single Photon Counting module (resolution 25 ps) to measure photon life
735 times. GFP fluorescence was imaged at the aequatorial plane of epidermis cells to
736 capture GFP fluorescence at the cell periphery and possibly plasma membrane. For
737 each interaction at least 10 cells were analysed in two replicates and a minimum of
738 1000 photons of the brightest pixel were recorded. Decay data within a region of
739 interest were fitted using an n-exponential reconvolution fit with model parameters
740 n=3 and measured instrument response function.

741 **Acknowledgements**

742 This work was supported by research grants from the German research foundation
743 (HU886/8 and SFB924) to RH. We are grateful to the TUM plant technology center
744 for support in propagation of barley plants.

745

746 **Conflict of interest**

747 The commercial use of RACB is regulated by patent WO 03020939.

748

749 **Supplemental Data**

750 **Suppl. Fig. S1: Barley RIC157 shows limited sequence similarity to RIC1 from**
751 ***Arabidopsis thaliana***

752 **Suppl. Fig. S2: RNA interference silencing efficiency**

753 **Suppl. Fig. S3: CRIB deletion and CRIB mutation in RIC157 prevents interaction**
754 **with RACB in yeast**

755 **Suppl. Fig. S4: Protein stability in yeast**

756 **Suppl. Figure S5: Raciometric BiFC analyses and BiFC fusion protein stability**

757 **Suppl. Fig. S6: RIC157 is recruited to the cell periphery by activated RACB**

758 **Suppl. Fig. S7: RIC157, recruited to the cell periphery by activated RACB,**
759 **colocalises with plasma membrane marker.**

760 **Suppl. Fig. S8: Barley RIC157 shows limited sequence similarity to RIC**
761 **proteins from *Arabidopsis thaliana*.**

762 **Suppl. Table 1: Primers used in this study**

763

764 **References**

765 **Akamatsu, A., Wong, H.L., Fujiwara, M., Okuda, J., Nishide, K., Uno, K., Imai, K.,**
766 **Umemura, K., Kawasaki, T., Kawano, Y. and Shimamoto, K. (2013). An**
767 **OsCEBiP/OsCERK1-OsRacGEF1-OsRac1 module is an essential early component**
768 **of chitin-induced rice immunity. Cell Host Microbe 13, 465-476.**

769

770 **Ash, J., Wu, C., Larocque, R., Jamal, M., Stevens, W., Osborne, M., Thomas,**
771 **D.Y. and Whiteway, M.** (2003). Genetic analysis of the interface between Cdc42p
772 and the CRIB domain of Ste20p in *Saccharomyces cerevisiae*. *Genetics* **163**, 9-20.

773

774 **Aspenström, P.** (1999). Effectors for the Rho GTPases. *Curr. Opin. Cell Biol.* **11**, 95-
775 102.

776

777 **Basu, D., Le, J., Zakharova, T., Mallery, E.L. and Szymanski, D.B.** (2008). A
778 SPIKE1 signaling complex controls actin-dependent cell morphogenesis through the
779 heteromeric WAVE and ARP2/3 complexes. *Proc. Natl. Acad. Sci. USA* **105**, 4044-
780 4049.

781

782 **Berken, A., Thomas, C. and Wittinghofer, A.** (2005). A new family of RhoGEFs
783 activates the Rop molecular switch in plants. *Nature* **436**, 1176-1180.

784

785 **Berken, A. and Wittinghofer, A.** (2008). Structure and function of Rho-type
786 molecular switches in plants. *Plant Physiol. Biochem.* **46**, 380-393.

787

788 **Białas, A., Zess, E.K., De la Concepcion, J.C., Franceschetti, M., Pennington,**
789 **H.G., Yoshida, K., Upson, J.L., Chanclud, E., Wu, C.-H., Langner, T., Maqbool,**
790 **A., Varden, F.A., Derevnina, L., Belhaj, K., Fujisaki, K., Saitoh, H., Terauchi, R.,**
791 **Banfield, M.J. and Kamoun, S.** (2018). Lessons in effector and NLR biology of
792 plant-microbe systems. *Mol. Plant Microbe Interact.* **31**, 34-45.

793

794 **Boller, T. and Felix, G.** (2009). A renaissance of elicitors: perception of microbe-
795 associated molecular patterns and danger signals by pattern-recognition receptors.
796 *Annu. Rev. Plant Biol.* **60**, 379-406.

797

798 **Boulter, E., and Garcia-Mata, R.** (2010). RhoGDI: A rheostat for the Rho switch.
799 *Small GTPases* **1**, 65-68.

800

801 **Brembu, T., Winge, P., Bones, A.M. and Yang, Z.** (2006). A RHOse by any other
802 name: a comparative analysis of animal and plant Rho GTPases. *Cell Res.* **16**, 435-
803 445.

804

805 **Burbelo, P.D., Drechsel, D. and Hall, A.** (1995). A conserved binding motif defines
806 numerous candidate target proteins for both Cdc42 and Rac GTPases. *J. Biol. Chem.*
807 **270**, 29071-29074.

808

809 **Chen, X. and Friml, J.** (2014). Rho-GTPase-regulated vesicle trafficking in plant cell
810 polarity. *Biochem. Soc. Trans.* **42**, 212-218.

811

812 **Cool, R.H., Schmidt, G., Lenzen, C.U., Prinz, H., Vogt, D. and Wittinghofer, A.**
813 (1999). The Ras mutant D119N is both dominant negative and activated. *Mol. Cell.*
814 *Biol.* **19**, 6297-6305.

815

816 **Craddock, C., Lavagi, I. and Yang, Z.** (2012). New insights into Rho signaling from
817 plant ROP/Rac GTPases. *Trends Cell Biol.* **22**, 492-501.

818

819 **Dangl, J.L., Horvath, D.M. and Staskawicz, B.J.** (2013). Pivoting the plant immune
820 system from dissection to deployment. *Science* **341**, 746-751.

821

822 **Douchkov, D., Nowara, D., Zierold, U. and Schweizer, P.** (2005). A high-
823 throughput gene-silencing system for the functional assessment of defense-related
824 genes in barley epidermal cells. *Mol. Plant Microbe Interact.* **18**, 755-761.

825

826 **Edgar, C.** (2004). MUSCLE: multiple sequence alignment with high accuracy and
827 high throughput. *Nucleic Acids Res.* **32**, 1792-1797.

828

829 **Engelhardt, S., Stam, R. and Hückelhoven, R.** (2018). Good riddance? Breaking
830 disease susceptibility in the era of new breeding technologies. *Agronomy* **8**, 114.

831

832 **Feiguelman, G., Fu, Y. and Yalovsky, S.** (2018). ROP GTPases structure-function
833 and signaling pathways. *Plant Physiol.* **176**, 57-79.

834

835 **Frantzeskakis, L., Kracher, B., Kusch, S., Yoshikawa-Maekawa, M., Bauer, S.,**
836 **Pedersen, C., Spanu, P.D., Maekawa, T., Schulze-Lefert, P. and Panstruga, R.**
837 (2018). Signatures of host specialisation and a recent transposable element burst in
838 the dynamic one-speed genome of the fungal barley powdery pathogen. *BMC*
839 *Genomics* **19**, 381.

840

841 **Fu, Y., Gu, Y., Zheng, Z., Wasteneys, G. and Yang, Z.** (2005). *Arabidopsis*
842 interdigitating cell growth requires two antagonistic pathways with opposing action on
843 cell morphogenesis. *Cell* **120**, 687-700.

844

845 **Fu, Y., Xu, T., Zhu, L., Wen, M. and Yang, Z.** (2009). A ROP GTPase signaling
846 pathway controls cortical microtubule ordering and cell expansion in *Arabidopsis*.
847 *Curr. Biol.* **19**, 1827-1832.

848

849 **Good, M.C., Zalatan, J.G. and Lim, W.A.** (2011). Scaffold proteins: Hubs for
850 controlling the flow of cellular information. *Science* **332**, 680-686.

851

852 **Gu, Y., Fu, Y., Dowd, P., Li, S., Vernoud, V., Gilroy, S. and Yang, Z.** (2005). A Rho
853 family GTPase controls actin dynamics and tip growth via two counteracting
854 downstream pathways in pollen tubes. *J. Cell Biol.* **169**, 127-138.

855

856 **Gu, Y., Li, S., Lord, E.M. and Yang, Z.** (2006). Members of a novel class of
857 *Arabidopsis* Rho guanine nucleotide exchange factors control Rho GTPase-
858 dependent polar growth. *Plant Cell* **18**, 366-381.

859

860 **Hahn, M. and Mendgen, K.** (2001). Signal and nutrient exchange at biotrophic plant-
861 fungus interfaces. *Curr. Opin. Plant Biol.* **4**, 322-327.

862

863 **Han, X. and Kahmann, R.** (2019). Manipulation of phytohormone pathways by
864 effectors of filamentous pathogens. *Front. Plant Sci.* **10**, 822.

865

866 **Hazak, O., Bloch, D., Poraty, L., Sternberg, H., Zhang, J., Friml, J. and Yalovsky,**
867 **S.** (2010). A rho scaffold integrates the secretory system with feedback mechanisms
868 in regulation of auxin distribution. *PLoS Biol.* **8**, e1000282.

869

870 **He, Q., Naqvi, S., McLellan, H., Boevink, P.C., Champouret, N., Hein, I. and**
871 **Birch, P.R.J.** (2018). Plant pathogen effector utilizes host susceptibility factor NLR1
872 to degrade the immune regulator SWAP70. *Proc. Natl. Acad. Sci. USA* **115**, E7834-
873 E7843.

874

875 **Higaki, T., Takigawa-Imamura, H., Akita, K., Kutsuna, N., Kobayashi, R.,**
876 **Hasezawa, S. and Miura, T.** (2017). Exogenous cellulase switches cell interdigitation
877 to cell elongation in an RIC1-dependent manner in *Arabidopsis thaliana* cotyledon
878 pavement cells. *Plant Cell Physiol.* **58**, 106-119.

879

880 **Hoefle, C., Huesmann, C., Schultheiss, H., Börnke, F., Hensel, G., Kumlehn, J.**
881 **and Hüchelhoven, R.** (2011). A barley ROP GTPase ACTIVATING PROTEIN
882 associates with microtubules and regulates entry of the barley powdery mildew
883 fungus into leaf epidermal cells. *Plant Cell* **23**, 2422-2439.

884

885 **Hoefle, C., McCollum, C. and Hückelhoven, R.** (2020). Barley ROP-Interactive
886 Partner-a organizes into RAC1- and MICROTUBULE-ASSOCIATED ROP-GTPASE
887 ACTIVATING PROTEIN 1-dependent membrane domains. *BMC Plant Biol.* **20**, 94.

888

889 **Hong, D., Jeon, B.W., Kim, S.Y., Hwang, J.-U. and Lee, Y.** (2016). The ROP2-
890 RIC7 pathway negatively regulates light-induced stomatal opening by inhibiting
891 exocyst subunit Exo70B1 in Arabidopsis. *New Phytol.* **209**, 624-635.

892

893 **Huesmann, C., Reiner, T., Hoefle, C., Preuss, J., Jurca, M.E., Domoki, M., Feher,
894 A. and Hückelhoven, R.** (2012). Barley ROP binding kinase 1 is involved in
895 microtubule organization and in basal penetration resistance to the barley powdery
896 mildew fungus. *Plant Physiol.* **159**, 311-320.

897

898 **Hückelhoven, R. and Panstruga, R.** (2011). Cell biology of the plant-powdery
899 mildew interaction. *Curr. Opin. Plant Biol.* **14**, 738-746.

900

901 **Inada, N. and Ueda, T.** (2014). Membrane trafficking pathways and their roles in
902 plant-microbe interactions. *Plant Cell Physiol.* **55**, 672-686.

903

904 **Jørgensen, J.H. and Wolfe, M.** (1994). Genetics of powdery mildew resistance in
905 barley. *Crit. Rev. Plant Sci.* **13**, 97-119.

906

907 **McKeen, W.E. and Rimmer, S.R.** (1973). Initial penetration process in powdery
908 mildew infection of susceptible barley leaves. *Phytopathology* **63**, 1049-1053.

909

910 **Kawano, Y., Akamatsu, A., Hayashi, K., Housen, Y., Okuda, J., Yao, A.,
911 Nakashima, A., Takahashi, H., Yoshida, H., Wong, H.L., Kawasaki, T. and**

912 **Shimamoto, K.** (2010). Activation of a Rac GTPase by the NLR family disease
913 resistance protein Pit plays a critical role in rice innate immunity. *Cell Host Microbe* **7**,
914 362-375.

915

916 **Kawano, Y., Fujiwara, T., Yao, A., Housen, Y., Hayashi, K. and Shimamoto, K.**
917 (2014). Palmitoylation-dependent membrane localisation of the rice resistance
918 protein Pit is critical for the activation of the small GTPase OsRac1. *J. Biol. Chem.*
919 **289**, 19079-19088.

920

921 **Klahre, U., Becker, C., Schmitt, A.C. and Kost, B.** (2006). Nt-RhoGDI2 regulates
922 Rac/Rop signaling and polar cell growth in tobacco pollen tubes. *Plant J.* **46**, 1018-
923 1031.

924

925 **Koh, S., Andre, A., Edwards, H., Ehrhardt, D. and Somerville, S.** (2005).
926 *Arabidopsis thaliana* subcellular responses to compatible *Erysiphe cichoracearum*
927 infections. *Plant J.* **44**, 516-529.

928

929 **Kushnirov, V.V.** (2000). Rapid and reliable protein extraction from yeast. *Yeast* **16**,
930 857-860.

931

932 **Kwaaitaal, M., Nielsen, M.E., Böhlenius, H. and Thordal-Christensen, H.** (2017).
933 The plant membrane surrounding powdery mildew haustoria shares properties with
934 the endoplasmic reticulum membrane. *J. Exp. Bot.* **68**, 5731-5743.

935

936 **Lavy, M., Bloch, D., Hazak, O., Gutman, I., Poraty, L., Sorek, N., Sternberg, H.**
937 **and Yalovsky, S.** (2007). A novel ROP/RAC effector links cell polarity, root-meristem
938 maintenance, and vesicle trafficking. *Curr. Biol.* **17**, 947-952.

939

940 **Lee, Y.J., Szumlanski, A., Nielsen, E. and Yang, Z.** (2008). Rho-GTPase-
941 dependent filamentous actin dynamics coordinate vesicle targeting and exocytosis
942 during tip growth. *J. Cell. Biol.* **181**, 1155-1168.

943

944 **Li, B. and Fields, S.** (1993). Identification of mutations in p53 that affect its binding to
945 SV40 large T antigen by using the yeast two-hybrid system. *FASEB J.* **7**, 957-963.

946

947 **Li, C., Lu, H., Li, W., Yuan, M. and Fu, Y.** (2017). A ROP2-RIC1 pathway fine-tunes
948 microtubule reorganization for salt tolerance in *Arabidopsis*. *Plant, Cell Environm.* **40**,
949 1127-1142.

950

951 **Lin, D., Cao, L., Zhou, Z., Zhu, L., Ehrhardt, D., Yang, Z. and Fu, Y.** (2013). Rho
952 GTPase signaling activates microtubule severing to promote microtubule ordering in
953 *Arabidopsis*. *Curr. Biol.* **23**, 290-297.

954

955 **McCollum, C., Engelhardt, S. and Hückelhoven, R.** (2019): ROP INTERACTIVE
956 PARTNER b interacts with the ROP GTPase RACB and supports fungal penetration
957 into barley epidermal cells. bioRxiv 750265.

958

959 **Meller, N., Merlot, S. and Guda, C.** (2005). CZH proteins: a new family of Rho-
960 GEFs. *J. Cell. Sci.* **118**, 4937-4946.

961

962 **Miklis, M., Consonni, C., Bhat, R.A., Lipka, V., Schulze-Lefert, P. and Panstruga,**
963 **R.** (2007). Barley MLO modulates actin-dependent and actin-independent antifungal
964 defense pathways at the cell periphery. *Plant Physiol.* **144**, 1132-1143.

965

966 **Mucha, E., Hoefle, C., Hückelhoven, R. and Berken, A.** (2010). RIP3 and
967 AtKinesin-13A – a novel interaction linking Rho proteins of plants to microtubules.
968 *Eur. J. Cell Biol.* **89**, 906-916.

969

970 **Nakashima, A., Chen, L., Thao, N.P., Fujiwara, M., Wong, H.L., Kuwano, M.,**
971 **Umemura, K., Shirasu, K., Kawasaki, T. and Shimamoto, K.** (2008). RACK1
972 functions in rice innate immunity by interacting with the Rac1 immune complex. *Plant*
973 *Cell* **20**, 2265-2279.

974

975 **Nelson, B.K., Cai, X. and Nebenführ, A.** (2007). A multicolored set of in vivo
976 organelle markers for co-localization studies in *Arabidopsis* and other plants. *Plant J.*
977 **51**, 1126-1136.

978

979 **Nibau, C., Wu, H.M. and Cheung, A.Y.** (2006). RAC/ROP GTPases: 'hubs' for
980 signal integration and diversification in plants. *Trends Plant Sci.* **11**, 309-315.

981

982 **Nottensteiner, M., Zechmann, B., McCollum, C., Hüchelhoven, R.** (2018). A
983 Barley powdery mildew fungus non-autonomous retrotransposon encodes a peptide
984 that supports penetration success on barley. *J. Exp. Bot.* **69**, 3745-3758.

985

986 **Opalski, K.S., Schultheiss, H., Kogel, K.H. and Hüchelhoven, R.** (2005). The
987 receptor-like MLO protein and the RAC/ROP family G-protein RACB modulate actin
988 reorganization in barley attacked by the biotrophic powdery mildew fungus *Blumeria*
989 *graminis* f.sp. *hordei*. *Plant J.* **41**, 291-303.

990

991 **Ostertag, M., Stammler, J., Douchkov, D., Eichmann, R. and Hüchelhoven, R.**
992 (2013). The conserved oligomeric Golgi complex is involved in penetration resistance
993 of barley to the barley powdery mildew fungus. *Mol. Plant Pathol.* **14**, 230-240.

994

995 **Panstruga, R. and Dodds, P.N.** (2009). Terrific protein traffic: The mystery of
996 effector protein delivery by filamentous plant pathogens. *Science* **324**, 748-750.

997

998 **Platre, M.P. et al.** (2019). Developmental control of plant Rho GTPase nano-
999 organization by the lipid phosphatidylserine. *Science* **364**, 57-62.

1000

1001 **Qin, L., Zhou, Z., Li, Q., Zhai, C., Liu, L., Quilichini, T.D., Gao, P., Kessler, S.A.,**
1002 **Jaillais, Y., Datla, R., Peng, G., Xiang, D. and Wei, Y.** (2020). Specific recruitment
1003 of phosphoinositide species to the plant-pathogen interfacial membrane underlies
1004 *Arabidopsis* susceptibility to fungal infection. *Plant Cell* **32**, 1665-1688.

1005

1006 **Reiner, T., Hoefle, C. and Hückelhoven, R.** (2016). A barley SKP1-like protein
1007 controls abundance of the susceptibility factor RACB and influences the interaction of
1008 barley with the barley powdery mildew fungus. *Mol. Plant Pathol.* **17**, 184-195.

1009

1010 **Ren, H., Dang, X., Cai, X., Yu, P., Li, Y., Zhang, S., Liu, M., Chen, B. and Lin, D.**
1011 (2017). Spatio-temporal orientation of microtubules controls conical cell shape in
1012 *Arabidopsis thaliana* petals. *PLoS Genet.* **13**, e1006851.

1013

1014 **Schaefer, A., Höhner, K., Berken, A. and Wittinghofer, A.** (2011). The unique
1015 plant RhoGAPs are dimeric and contain a CRIB motif required for affinity and
1016 specificity towards cognate small G proteins. *Biopolymers* **95**, 420-433.

1017

1018 **Scheler, B., Schnepf, V., Galgenmüller, C., Ranf, S. and Hückelhoven, R.** (2016).
1019 Barley disease susceptibility factor RACB acts in epidermal cell polarity and
1020 positioning of the nucleus. *J. Exp. Bot.* **67**, 3263-3275.

1021

1022 **Schnepf, V., Vlot, C.A., Kugler, K. and Hückelhoven, R.** (2018). Barley
1023 susceptibility factor RACB modulates transcript levels of signalling protein genes in
1024 compatible interactions with *Blumeria graminis* f.sp. *hordei*. *Mol. Plant Pathol.* **19**,
1025 393-404.

1026

1027 **Schultheiss, H., Dechert, C., Kogel, K.-H. and Hüchelhoven R.** (2002). A small
1028 GTP-binding host protein is required for entry of powdery mildew fungus into
1029 epidermal cells of barley. *Plant Physiol.* **128**, 1447-1454.

1030

1031 **Schultheiss, H., Dechert, C., Kogel, K.-H. and Hüchelhoven, R.** (2003). Functional
1032 analysis of barley RAC/ROP G-protein family members in susceptibility to the
1033 powdery mildew fungus. *Plant J.* **36**, 589-601.

1034

1035 **Schultheiss, H., Preuss, J., Pircher, T., Eichmann, R. and Hüchelhoven, R.**
1036 (2008). Barley RIC171 interacts with RACB *in planta* and supports entry of the
1037 powdery mildew fungus. *Cell. Microbiol.* **10**, 1815-1826.

1038

1039 **Schulze-Lefert, P. and Vogel, J.** (2000). Closing the ranks to attack by powdery
1040 mildew. *Trends in Plant Science* **5**, 343-348.

1041

1042 **Schweizer, P., Christoffel, A. and Dudler, R.** (1999). Transient expression of
1043 members of the germin-like gene family in epidermal cells of wheat confers disease
1044 resistance. *Plant J.* **20**, 541-552.

1045

1046 **Spanu, P.D. et al.** (2010). Genome expansion and gene loss in powdery mildew
1047 fungi reveal tradeoffs in extreme parasitism. *Science* **330**, 1543-1546.

1048

1049 **Stukenbrock, E.H., McDonald, B.A.** (2009) Population genetics of fungal and
1050 oomycete effectors involved in gene-for-gene interactions. *Mol Plant Microbe*
1051 *Interact.*

1052 22, 371-380.

1053

1054 **Sugiyama, Y., Nagashima, Y., Wakazaki, M., Sato, M., Toyooka, K., Fukuda, H.**
1055 **and Oda, Y.** (2019). A Rho-actin signaling pathway shapes cell wall boundaries in
1056 *Arabidopsis* xylem vessels. *Nat. Commun.* **10**, 468.

1057

1058 **Vickers, C.E., Xue, G.P. and Gresshoff, P.M.** (2003). A synthetic xylanase as a
1059 novel reporter in plants. *Plant Cell Rep.* **22**, 135-140.

1060

1061 **Voegelé, R.T., Struck, C., Hahn, M. and Mendgen, K.** (2001). The role of haustoria
1062 in sugar supply during infection of broad bean by the rust fungus *Uromyces fabae*.
1063 *Proc. Natl. Acad. Sci. USA* **98**, 8133-8138.

1064

1065 **Waadt, R., Schmidt, L.K., Lohse, M., Hashimoto, K., Bock, R. and Kudla, J.**
1066 (2008). Multicolor bimolecular fluorescence complementation reveals simultaneous
1067 formation of alternative CBL/CIPK complexes *in planta*. *Plant J.* **56**, 505-516.

1068

1069 **Walter, M., Chaban, C., Schütze, K., Batistic, O., Weckermann, K., Näke, C.,**
1070 **Blazevich, D., Grefen, C., Schumacher, K., Oecking, C., Harter, K. and Kudla, J.**
1071 (2004). Visualization of protein interactions in living plant cells using bimolecular
1072 fluorescence complementation. *Plant J.* **40**, 428-438.

1073

1074 **Wang, Q., Li, Y., Ishikawa, K., Kosami, K.I., Uno, K., Nagawa, S., Tan, L., Du, J.,**
1075 **Shimamoto, K. and Kawano, Y.** (2018). Resistance protein Pit interacts with the
1076 GEF OsSPK1 to activate OsRac1 and trigger rice immunity. *Proc. Natl. Acad. Sci.*
1077 *USA* **115**, E11551-E11560.

1078

1079 **Wicker, T. et al.** (2013). The wheat powdery mildew genome shows the unique
1080 evolution of an obligate biotroph. *Nat. Genet.* **45**, 1092-1096.

1081

1082 **Wu, G., Gu, Y., Li, S. and Yang, Z.** (2001). A genome-wide analysis of Arabidopsis
1083 Rop-interactive CRIB motif-containing proteins that act as ROP GTPase targets.
1084 *Plant Cell* **13**, 2841-2856.

1085

1086 **Wu, H., Hazak, O., Cheung, A.Y. and Yalovsky, S.** (2011). RAC/ROP GTPases and
1087 auxin signaling. *Plant Cell* **23**, 1208-1218.

1088

1089 **Yalovsky, S.** (2015). Protein lipid modifications and the regulation of ROP GTPase
1090 function. *J. Exp. Bot.* **66**, 1617-1624.

1091

1092 **Yalovsky, S., Bloch, D., Sorek, N. and Kost, B.** (2008). Regulation of membrane
1093 trafficking, cytoskeleton dynamics, and cell polarity by ROP/RAC GTPases. *Plant*
1094 *Physiol.* **147**, 1527-1543.

1095

1096 **Yamaguchi, K. and Kawasaki, T.** (2012). Function of Arabidopsis SWAP70 GEF in
1097 immune response. *Plant Signal Behav.* **7**, 465-468.

1098

1099 **Yamaguchi, K., Imai, K., Akamatsu, A., Mihashi, M., Hayashi, N., Shimamoto, K.**
1100 **and Kawasaki, T.** (2012). SWAP70 functions as a Rac/Rop guanine nucleotide-
1101 exchange factor in rice. *Plant J.* **70**, 389-397.

1102

1103 **Zeke, A., Lukacs, M., Lim, W.A. and Remenyi, A.** (2009). Scaffolds: interaction
1104 platforms for cellular signalling circuits. *Trends Cell Biol.* **19**, 364-374.

1105

1106 **Zhang, Y., Xiong, Y., Liu, R., Xue, H.W. and Yang, Z.** (2019). The Rho-family
1107 GTPase *OsRAC1* controls rice grain size and yield by regulating cell division. *Proc.*
1108 *Natl. Acad. Sci. USA* **116**, 16121-16126.

1109

1110 **Zhou, Z., Shi, H., Chen, B., Zhang, R., Huang, S. and Fu, Y.** (2015). Arabidopsis
1111 RIC1 severs actin filaments at the apex to regulate pollen tube growth. *Plant Cell* **27**,
1112 1140-1161.

1113

1114 **Zhou, Z., Pang, Z., Zhao, S., Zhang, L., Lv, Q., Yin, D., Li, D., Xue, L., Zhao, X., Li,**
1115 **X., Wang, W. and Zhu, L.** (2019). Importance of OsRAC1 and RAI1 in signalling of
1116 nucleotide-binding site leucine-rich repeat protein-mediated resistance to rice blast
1117 disease. *New Phytol.* **223**, 828-838.

1118

1119 **Figures**

1120

1121 **Figure 1: Barley RIC proteins alignment.** Multiple alignment
1122 (<https://www.ebi.ac.uk/Tools/msa/muscle>, Edgar 2004; illustrated using Jalview
1123 2.11.0 software) of predicted barley (*Hordeum vulgare*, Hv) proteins harboring CRIB
1124 domain (underlined). Intensity of blue coloured amino acids represents level of
1125 conservation (higher intensity = more conserved). CRIB domain consensus
1126 sequence of barley RIC proteins is indicated by coloured amino acid sequence above
1127 the alignment (<http://meme-suite.org/tools/meme>).

1128

1129

1130 **Figure 2: RIC157 increases susceptibility in a RACB-dependent manner.**

1131 Epidermal cells of 7 day old primary barley leaves were transiently transformed by
1132 particle bombardment with either (A) an overexpression construct of RIC157, (B) a
1133 RNA interference construct of RIC157, (C) simultaneously with an overexpression
1134 construct of RIC157 and a RNA interference construct of RACB or (D) an
1135 overexpression construct of RIC157 N-terminally tagged with GFP. Empty
1136 overexpression or RNA interference plasmids were used as controls (-ve). The
1137 penetration efficiency of *Bgh* into transformed barley epidermal cells was analysed
1138 48h after inoculation with fungal spores. Values are shown as mean of at least 3
1139 independent biological replicates, relative to the mean of the control set as 100%. **
1140 indicates significance $P < 0.01$, Student's t-test.

1141

1142

1143 **Figure 3: RIC157 interacts directly with RACB in yeast and in planta.** A) Yeast-2-

1144 Hybrid indicates direct interaction between RIC157 and RACB in yeast. Yeast strain
1145 AH109 was transformed with indicated bait and prey fusion constructs. Overnight
1146 cultures of yeast transformants were dropped onto Complete Supplement Medium
1147 plates either lacking leucine and tryptophan (LW) or lacking leucine, tryptophan and
1148 adenin (LWAde) and incubated at 30°C. Growth on LWAde medium indicates
1149 interaction between bait and prey fusion proteins. -ve denotes empty prey and bait
1150 plasmid. Photos were taken 2 days (LW) and 7 days (LWAde), respectively, after
1151 dropping. B) Quantification of FLIM analysis confirms direct protein-protein interaction
1152 between RIC157 and RACB *in planta*. GFP lifetime in barley epidermal cells

1153 transiently co-expressing indicated constructs was investigated at the aequatorial
1154 plane 2d after transformation via particle bombardment. Graph shows result of 2
1155 independent biological replicates. **** indicates significance $P < 0.0001$, Student's t-
1156 test.

1157

1158

1159 **Figure 4: RIC157 localisation is affected by RACB-activation status.** Confocal
1160 scanning microscopy of barley epidermal cells 1d after transformation via particle
1161 bombardment. A) GFP-RIC157 localises to the cytoplasm, but not the nucleus (upper
1162 row) and is recruited to the cell periphery exclusively by mCherry-CARACB(G15V),
1163 but not by mCherry-RACB or mCherry-DNRACB(D121N). B) Simultaneous RNA
1164 interference-mediated silencing of RACB attenuates RIC157 recruitment to the cell
1165 periphery. Arrows indicate cytoplasmic strands, arrow heads point towards GFP
1166 fluorescence accumulation at cell periphery. Microscopy pictures show maximum
1167 projections of at least 15 optical sections taken at 2 μ m increments. Bar = 50 μ m.

1168

1169

1170 **Figure 5: RIC157 is recruited to penetration site where it colocalises with**
1171 **activated RACB.** Confocal laser scanning microscopy of epidermal cells 1d after
1172 transformation via particle bombardment and 18-24h after inoculation with *Bgh*. Cells
1173 in A) and B) show successful fungal penetration due to haustorium formation (h). A)
1174 Transient co-expression of GFP-CARACB(G15V) and mCherry-RIC157. Area in
1175 white square is enlarged in lower panel. S = spore; Bar = 30 μ m. B) Transient co-
1176 expression of CFP-CARACB(G15V) and GFP-RIC157. Cytosolic mCherry was
1177 expressed to distinguish RIC157 and CARACB(G15V) localisation from cytoplasm at
1178 penetration site. Bar = 20 μ m. Arrows indicate approximate position of the haustorial
1179 neck. Contrast of images was equally slightly enhanced. Arrows indicate haustorial
1180 neck close to fungal penetration site.

1181

1182

1183 **Suppl. Fig. S1: Barley RIC157 shows limited sequence similarity to barley**
1184 **RIC168 and RIC171, but also to RIC proteins from *Arabidopsis thaliana* and**
1185 ***Oryza sativa*.** Primary sequences of RIC proteins (schematically shown in top part of
1186 the figure) were analysed for domain homologies using MEME online software
1187 (<http://meme-suite.org/tools/meme>). Consensus sequence of the four most similar
1188 motifs are shown below. Underlined sequence denotes CRIB domain. Hv = *Hordeum*
1189 *vulgare*, At = *Arabidopsis thaliana*, Os = *Oryza sativa*.

1190

1191

1192 **Suppl. Fig. S2: RNA interference-mediated silencing efficiency.** Epidermal cells
1193 of 7d old barley primary leaves were transiently transformed via particle
1194 bombardment with overexpression constructs of GFP fusions of RIC157 (A) and
1195 RACB (B) alone or together with RNAi silencing constructs. A construct to express
1196 cytosolic mCherry was simultaneously co-delivered for transformation efficiency and
1197 fluorescence quantification purposes. Microscopy images are maximum projections
1198 of at least 15 optical sections taken at 2µm increments. Bars = 50µm. Each graph
1199 shows the mean of GFP fluorescence as percentage of mCherry fluorescence per
1200 transformed cell (whole cell area was taken as region of interest for measuring
1201 fluorescence intensity). Dots represent single measured cells. **** indicates
1202 significance $P < 0.0001$

1203

1204

1205 **Suppl. Fig. S3: CRIB deletion and CRIB mutation in RIC157 prevents interaction**
1206 **with RACB in yeast.** Yeast strain AH109 was transformed with indicated bait and
1207 prey fusion constructs. Overnight cultures of yeast transformants were dropped onto
1208 Complete Supplement Medium plates either lacking leucine and tryptophan (LW) or
1209 lacking leucine, tryptophan and adenin (LWAde) and incubated at 30°C. Growth on
1210 LWAde medium indicates interaction between bait and prey fusion proteins. –ve
1211 denotes empty prey and bait plasmid. Photos were taken 2 days (LW) and 7 days
1212 (LWAde), respectively, after dropping.

1213

1214

1215 **Suppl. Fig. S4: Protein stability in yeast.** Immunoblots probed with α -cMyc to
1216 detect RACB variants fused to GAL4 binding domain (BD; bait) encoded on pGBKT7
1217 and α -HA to detect RIC157 variants fused to GAL4 activation domain (AD; prey)
1218 encoded on pGADT7 after transformation of yeast strain AH109. Total yeast protein
1219 was extracted as described in Experimental Procedures. Molecular weight is
1220 indicated in kiloDalton (kDA). Ponceau S staining shows protein loading. Stable
1221 expression of RIC157 variants fused to GAL4 activation domain could not be
1222 detected in immunoblots (arrow indicates expected bandsize).

1223

1224

1225 **Suppl. Figure S5: Ratiometric BiFC analyses and BiFC fusion protein stability.**

1226 A) Barley epidermal cells were transiently transformed with indicated constructs
1227 encoding for BiFC fusion proteins. Cytosolic mCherry expression was used in each
1228 sample as transformation marker and to quantify reconstituted YFP fluorescence
1229 ratiometrically. The whole cell area was taken as region of interest. Graph shows the
1230 mean of the YFP/mCherry fluorescence ratio, taken from at least 20 cells (shown as
1231 dots. **** indicates significance $P < 0.0001$, ** indicates significance $P < 0.01$
1232 Student's t-test. B) Barley mesophyll protoplasts were prepared and transformed with
1233 BiFC constructs as described in Experimental procedures. To confirm stable *in planta*
1234 expression, immunoblots were probed with α -HA to detect YFPc-RACB fusion
1235 proteins and α -cMyc to detect YFPn-RIC157 fusion proteins. Ponceau S staining
1236 shows equal protein loading. C) BiFC shows close proximity between RIC157 and
1237 RACB *in planta*. Barley epidermal cells transiently co-expressing split-YFP fusion
1238 protein combinations and mCherry as cytosolic transformation marker after particle
1239 bombardment transformation. 2d after transformation, YFP fluorescence
1240 reconstitution was analysed via Confocal laser scanning microscopy. Shown are
1241 maximum projections of at least 15 optical sections taken at 2 μ m increments. Bars =
1242 50 μ m.

1243

1244

1245

1246

1247 **Suppl. Fig. S6: RIC157 is recruited to the cell periphery by activated RACB.**

1248 Confocal laser scanning microscopy of barley epidermal cells 1d after transient

1249 transformation via particle bombardment. GFP-RIC157 localises to the cytoplasm,
1250 but not the nucleus and is recruited to the cell periphery exclusively by non-tagged
1251 CARACB(G15V), but not DNRACB(D121N). A construct for cytosolic mCherry
1252 expression was simultaneously used to check transformation efficiency. Arrows
1253 indicate cytoplasmic strands, arrow heads point towards GFP fluorescence
1254 accumulation at cell periphery. Microscopy pictures show maximum projections of at
1255 least 15 optical sections taken at 2µm increments. Bar = 50µm.

1256

1257

1258 **Suppl. Fig. S7: RIC157, recruited to the cell periphery by activated RACB,**
1259 **colocalises with plasma membrane marker.** Confocal laser scanning microscopy
1260 of barley epidermal cells 1d after transient transformation via particle bombardment
1261 to express GFP-RIC157, red-fluorescent plasma membrane marker pm-rk (Nelson *et*
1262 *al.*, 2007) and non-tagged CARACB(G15V). Microscopy pictures show A) maximum
1263 projections of at least 15 optical sections taken at 2µm increments to visualize global
1264 recruitment of GFP-RIC157 to the cell periphery in the presence of activated RACB
1265 or B) and C) a single optical section to confirm specific colocalisation of GFP-RIC157
1266 with plasma membrane marker pm-rk. B) and C) show overlay analysis of both
1267 fluorescences in the absence or presence of overexpressed CARACB(G15V), either
1268 via magnification (inset in upper panel) or via graphical visualization of fluorescence
1269 signal intensities (lower panel) measured over a region of interest (white line in
1270 middle panel). Bar = 50µm.

1271

1272

1273

1274

1275 **Suppl. Fig. S8: Barley RIC157 shows limited sequence similarity to RIC**
1276 **proteins from *Arabidopsis thaliana*.** Primary sequences of RIC proteins
1277 (schematically shown in top part of the figure) were analysed for domain homologies
1278 using MEME online software (<http://meme-suite.org/tools/meme>). Consensus
1279 sequence of the four most similar motifs are shown below. Underlined sequence
1280 denotes CRIB domain. Hv = *Hordeum vulgare*, At = *Arabidopsis thaliana*.

1281

1282 **Suppl. Table 1: Primers used in this study**

Primer name	Gene (construct)	Sequence
RIC157_GW_for	<i>RIC157</i>	5'-AAAAAGCAGGCTCACAAATGGCGGTAAAGATGAAGGG-3'
RIC157_GW_rev+STOP	<i>RIC157</i>	5'- AGAAAGCTGGGTCAACCGCTCCGGATCAGACGACTCGAACCCCTCTT TGC-3'
RIC157delCRIB_for	<i>RIC157ΔCRIB</i>	5'-GCTCAAAGGAGCATGAGATGGAATTGGGCACCAGTGACACATC- 3'
RIC157delCRIB_rev	<i>RIC157ΔCRIB</i>	5'-CACTGGTGCCCAATTCCATCTCATGCTCCTTTGAGC-3'
CRIB157H37&40Y_for	<i>RIC157-H37-40Y</i>	5'- CCTACAGATGTAAAGTATGTGGCTTACATAGTTTGGGCACCAGTGA CACATCTCC-3'
CRIB157H37&40Y_rev	<i>RIC157-H37-40Y</i>	5'- GGAGATGTGCTACTGGTGCCCAAACCTATGTAAGCCACATACTTTAC ATCTGTAGG-3'
attB1	<i>attB1</i>	5'-GGGGACAAGTTTGTACAAAAAGCAGGCTCACAA-3'
attB2	<i>attB2</i>	5'-GGGGACCACTTTGTACAAGAAAGCTGGGTCAACCG-3'
RIC157_RNAi_NotI_for	<i>RIC157 RNAi</i>	5'-AATTGCGGCCCAAGATGAAGGGAATCTTCAAAGGGC -3'
RIC157_RNAi_XbaI_rev	<i>RIC157 RNAi</i>	5'-AATTTCTAGAACGCCGTGCGAAGGAGGCCCTCGACC -3'
RIC157_RNAi_EcoRI_for	<i>RIC157 RNAi</i>	5'-AATTGAATTCTTGGGCACCAGTGACACATCTCC-3'
RIC157_RNAi_EcoRI_rev	<i>RIC157 RNAi</i>	5'-AATTGAATTCTTCCATCTCATGCTCCTTTTGGAGC-3'
RIC157_BamHI_for	<i>RIC157</i>	5'-AATTGGATCCATGGCGGTAAAGATGAAGGGAATC-3'
RIC157_KpnI_rev	<i>RIC157</i>	5'-AATTGGTACCCTAGACGACTCGAACCCCTCTTTGC-3'
RIC157_for	<i>RIC157</i>	5'-ATGGCGGTAAAGATGAAGG-3'
RIC157_rev	<i>RIC157</i>	5'-GACGACTCGAACCCCTCTTTGC-3'
RACB_D121N_fw	<i>DNRACB(D121N)</i>	5'-CTCGTGGGAACAAAGCTTAATCTTCGAGATGACAAG-3'
RACB_D121N_rv	<i>DNRACB(D121N)</i>	5'-CTTGTCATCTCGAAGATTAAGCTTTGTTCCACGAG-3'
RACB_GW_for	<i>RACB</i>	5'-AAAAAGCAGGCTCACAAATGAGCGCGTCCAGGTTTATAAAGTGC-3'
RACB_GW_rev	<i>RACB</i>	5'- AGAAAGCTGGGTCAACCGCTCCGGACAAGATGGAGCAAGCCCCC- 3'
HvUBC2_fwd	<i>Ubiquitin conjugating enzyme 2</i>	5'-TCTCGTCCCTGAGATTGCCACAT-3'
HvUBC2_rev	<i>Ubiquitin conjugating enzyme 2</i>	5'-TTTCTCGGGACAGCAACACAATCTTCT-3'
delCSIL_for	<i>RACBΔCSIL</i>	5'- GAAGAAAAAGGCGCAGAGGGGGGCTTGATCCATCTTGTAGTCCGGA GGCGGTG-3'
delCSIL_rev	<i>RACBΔCSIL</i>	5'- CACCGCTCCGACTACAAGATGGATCAAGCCCCCTCTGCGCCTT TTCTTC-3'
GW_RfA_mCherry-F	<i>mCherry</i>	5'-GCTGTACAAGATCACAAAGTTTGTACAAAAAGCTG-3'
GW_RfA_meGFP-F	<i>meGFP</i>	5'-GCTGTACAAAATCACAAAGTTTGTACAAAAAGCTG-3'
GW_RfA_Xba-R	<i>RfA</i>	5'- TGCCTGCAGGTGCGACTCTAGAATCACCCTTTGTACAAGAAAGCTG-3'

GW_Xba_RfB-F	<i>RfB</i>	5'- GGTACCCGGGGATCCTCTAGAATCAACAAGTTTGTACAAAAAGCT-3'
GW_RfB-R	<i>RfB</i>	5'-TGCTCACCATATCAACCACTTTGTACAAGAAAGCT-3'
meGFP-STP-F	<i>meGFP</i>	5'-AGTGTTGATATGGTGAGCAAGGGCGAGG-3'
mCherry-STP-F	<i>mCherry</i>	5'-AGTGTTGATATGGTGAGCAAGGGCGAGG-3'
XFP-noSTP_Xba-F	<i>XFP</i>	5'-GGTACCCGGGGATCCTCTAGAATGGTGAGCAAGGGCGAGG-3'
XFP-noSTP-R	<i>XFP</i>	5'-AACTTGTGATCTTGTACAGCTCGTCCATGCC-3'
meGFP-noSTP-R	<i>meGFP</i>	5'-AACTTGTGATTTTGTACAGCTCGTCCATGCC-3'
mCherry-STP_Xba-R	<i>mCherry</i>	5'-TGCCTGCAGGTCGACTCTAGATTACTTGTACAGCTCGTCCATGCC- 3'
meGFP-STP_Xba-R	<i>meGFP</i>	5'-TGCCTGCAGGTCGACTCTAGATTATTTGTACAGCTCGTCCATGCC- 3'

1283

HvRIC163	1	MKDRRAGAGFPFSIGCMSQSAVAVADPLEKKPMPPPPAQQQADTPSSSTTAATTQERSAGEESGEDKARNAAASG-IVSAG	80
HvRIC153	1	-----MASISTDDAAPTSHVDAPVPVATGDHEEAAGVVGKGTASAEQAAARRDVFLLAG	54
HvRIC170	1	-----MKG	3
HvRIC194	1	-----MGSREQQRGRDRFIVIPFSSTCRSAASVDIVQSKKPQGAGGGGEGTSAAAVVRPAKG-ESLSL	63
HvRIC236	1	-----MST-KMKKG	8
HvRIC157	1	-----MA-VKMKG	7
HvRIC171	1	-----MASN-YKMKG	9
HvRIC168	1	-----MA-YKMKG	7

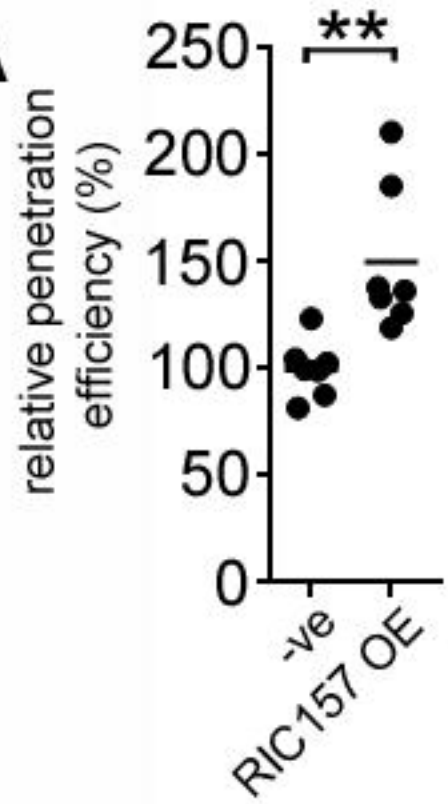
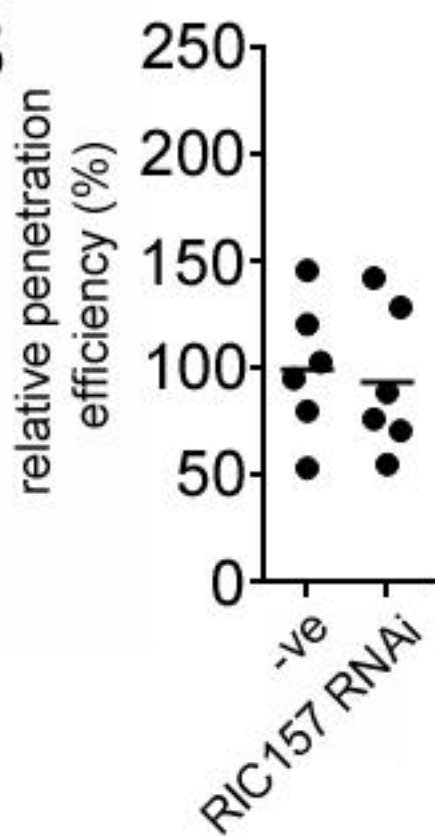
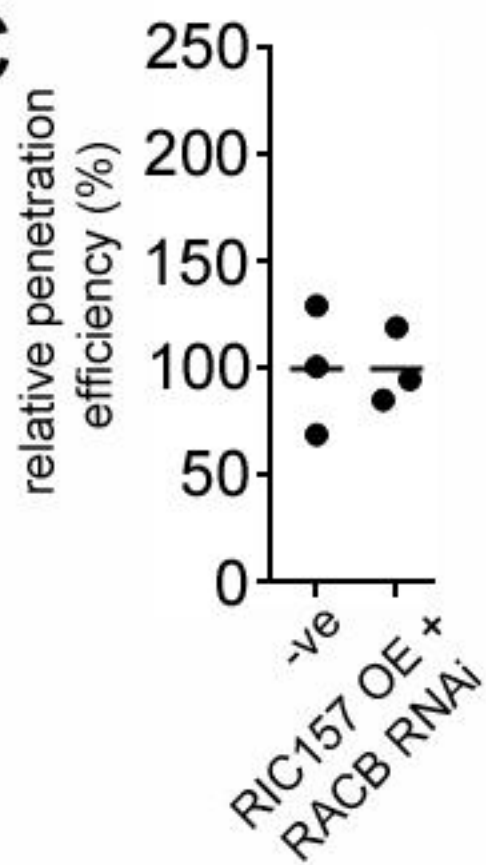
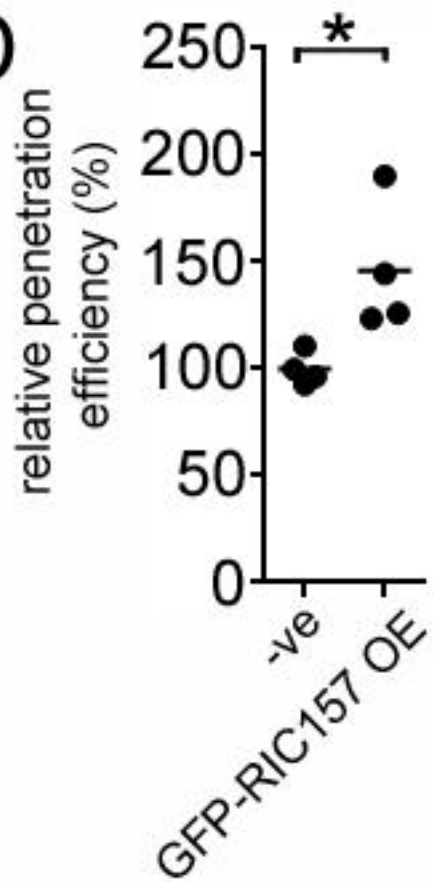
IGPTDVKHVAHIG

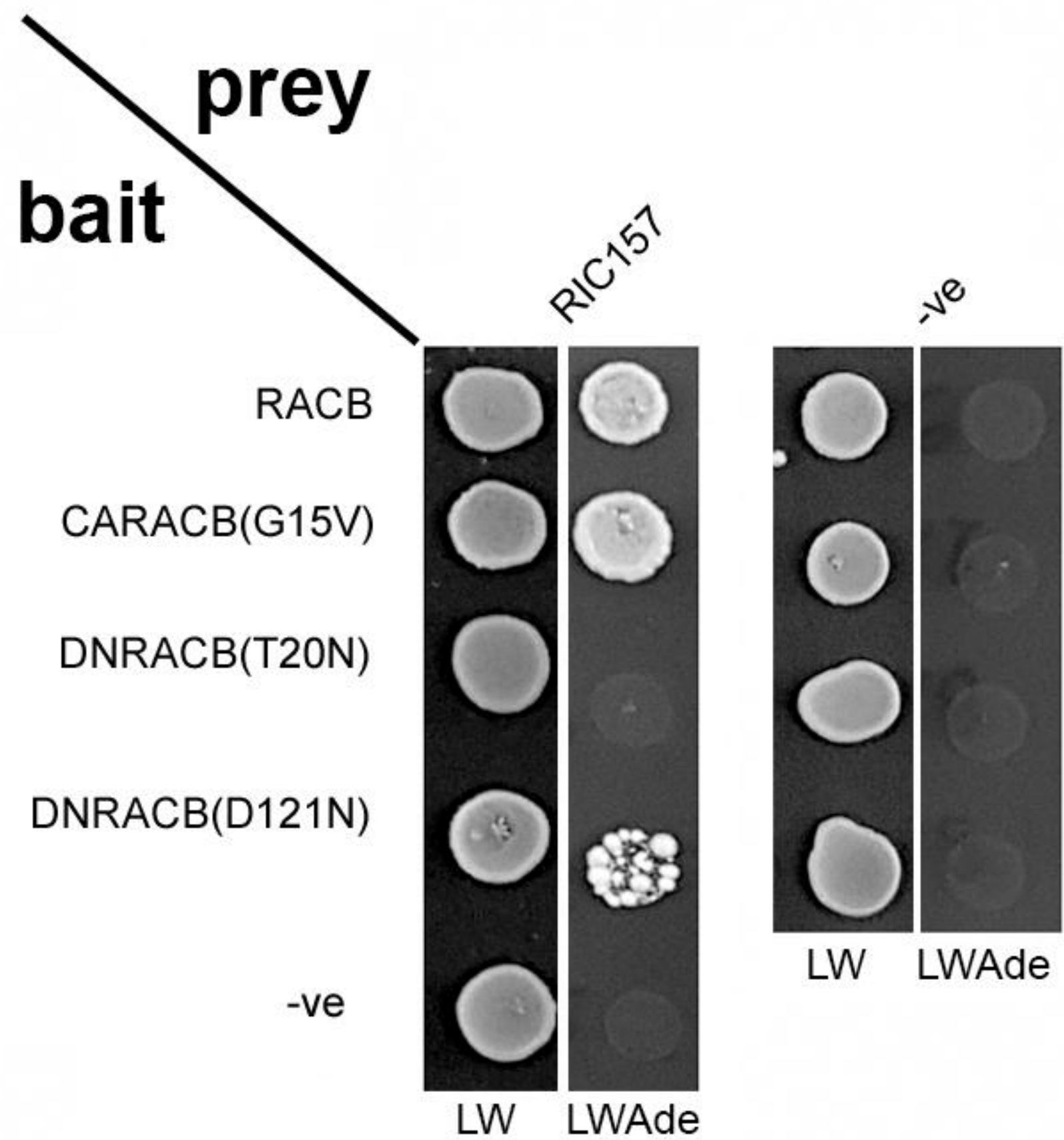
HvRIC163	81	VQRL LKGIKT----FFAAYDGEEDDEAEIVIGFPTDVQHVGHIGWDGIN-----	128
HvRIC153	55	IRKLIKSFRLTH-IFEMYEDGDEEDDDDIQIGFPTDVEHVAHIGLDGSS-----SVA----	108
HvRIC170	4	L---LKGLRYISQ-IFDP-----KEP--EIQIGAPTDVKHVAHIGWDNNS-----VANPAWMSEFKAQPGASGSGGP	64
HvRIC194	64	VARL LRGFKNLSHQIFAVYDEDEDEEPE--EMVIGLPTDVKHVAHIGWDGST---STTSSVRSW-----NRAAPP	129
HvRIC236	9	I---LRPFYFSN-IDA-----KEQ--DMQIGFPTDVKHVAHIGWDGSPVNPKEKEAGAPSWMKDYHSAPLDSASFRS	76
HvRIC157	8	I---FKGLRIFSH-MFAA-----QKEH--EMEIGFPTDVKHVAHIGLGTSD-----TSPSWMNEFKSSE-DLSAGSL	67
HvRIC171	10	F---FKGFKIISQ-IFAA-----KEQ--EMVIGRPTDVKHVAHIGWSSST-PGTLTGNASPSWMNVEGSS-DFS--SM	73
HvRIC168	8	V---FKGLRVITQ-IFVV-----KEQ--EMEIGYPI DVKHVAHIGWDSPT--GSAATSPTPSWMNDMKGTP-DIS--TL	70

CRIB

HvRIC163	129	-----KVGGMVGAFLSP-----	140
HvRIC153	109	-----SLRGMDGARELLSLS-----	123
HvRIC170	65	EGAEQPGGGGGGAGKAE---QSEAKPRRTRGKGS GGAEGKRDVSRRP-----AKTEGSAE	117
HvRIC194	130	GTTAPAAASASTS-----ASASSSSAAPPQPQA-----	157
HvRIC236	77	DRGGSAAASNPWASQEIVLDGAGLGDNSFRDTKSEAGGIEVTAGDSPSPGTRRSRRNRSRGSDTSSMDVTTGITDTSEKKE	157
HvRIC157	68	STAEQSRQTSWTSDFEP-----ARSMLPTEINFDRP-----AQE	103
HvRIC171	74	GYFAPSAGTSWTSQDFEQHHQPPRDMLPLG IASEITGEDVAAAPYDPV-----	122
HvRIC168	71	SNSGPSTGTSWSQDFDH---PRDISAYGII--PENSSPGATPYDIP-----	113

HvRIC163	141	----SSLSLR--QLEIAMDPGASTTTCIN-----	163
HvRIC153	124	----TNISLH--QFEFAMASIAAHDRSS-----AAITASP-----	153
HvRIC170	118	AGEGDAAAPKQ-RRRKSKTAGGASGGRSK-----SGSGGAASDPEAAKSASAEADDDGR-----	170
HvRIC194	158	--QPPSLSAR--QFELAMAAQASAAATTS-----TSGAARRHRHYS-----	194
HvRIC236	158	KAKKGTRKNR--KKDKDKATEDTAGSTCQDLPAVPKKSNNRRKNKGSSEGGSGASTKDGGGVPEEGTTPLTLVAEEEEKDHEL	236
HvRIC157	104	SSSCP PRGPRKARRKKTRTSSPTSSARSS-----SSRSRASFAFDDFSESQRGVRVV-----	157
HvRIC171	123	--RPPPRKTR--RKKKT VVGSLVNSSVTN-----DSSASAS--TVATRVD AIDTNSVIS-----	171
HvRIC168	114	--KPPRRPR--RKKSSKNSSPTASTRSS-----RSSRSRSKGSLSSTTPDTIGANDTQREIQIL-----	168

A**B****C****D**

A**B**